

AN INVESTIGATION OF THE BURSTING EVENTS IN
DRAG REDUCING TURBULENT CHANNEL FLOWS

By

ALAN JACKSON SMITH

Bachelor of Science

Oklahoma State University

Stillwater, Oklahoma

1973

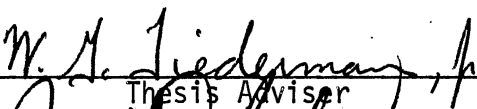
Submitted to the Faculty of the Graduate College
of the Oklahoma State University
in partial fulfillment of the requirements
for the Degree of
MASTER OF SCIENCE
December, 1975

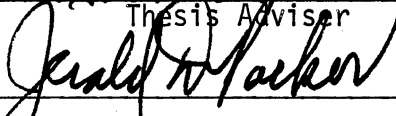
Thesis
1975
5642i
cop.2

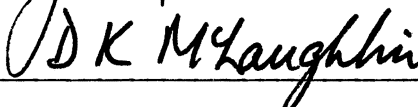
MAR 24 1976

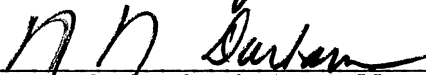
AN INVESTIGATION OF THE BURSTING EVENTS IN
DRAG REDUCING TURBULENT CHANNEL FLOWS

Thesis Approved:



Thesis Adviser






Dean of the Graduate College

935091

ACKNOWLEDGMENTS

I would like to thank my adviser, Professor William G. Tiederman, for the excellent guidance which he has personally provided me throughout this study. I would also like to thank Professors Dennis K. McLaughlin and Jerald D. Parker for the valuable comments and discussion which they have generously provided throughout this study.

A special thank you goes to Mr. David Oldaker for his general helpfulness in actually accomplishing the experiments described in this study. Thanks also go to Mr. Afshin Ghajar and Mr. Scott Quigley.

This study was financed partially through National Science Foundation Grant GK-40609, partially through a Graduate Research Assistantship provided by the School of Mechanical and Aerospace Engineering, Oklahoma State University, and partially through the generous assistance of Mr. and Mrs. Earl B. Smith. This assistance is appreciated.

Thanks also go to Dow Chemical Corporation and Halliburton Services for their generous contributions of polymer, Ms. Charlene Fries for typing the final manuscript, and Mr. Lynn Alger for his excellent art work.

TABLE OF CONTENTS

Chapter	Page
I. INTRODUCTION	1
Objectives	5
II. EXPERIMENTAL PROCEDURE	7
Experimental Apparatus	7
Polymer Solutions	8
Preparation of Polymer Solutions	9
Drag Reduction	10
Channel Wall Shear Stress and Mass Averaged Velocity Measurements	10
Flow Visualization	11
Data Reduction	12
III. EXPERIMENTAL RESULTS	15
Test to Demonstrate Feasibility of Method II	15
Bursting Period Measurements	17
Bursting Period Durations	22
IV. DISCUSSION	24
Measurement Technique	24
Bursting Period Correlations	25
Structural Changes Occurring in Drag Reducing Flows . .	27
V. CONCLUSIONS AND RECOMMENDATIONS	28
Conclusions	28
Recommendations	29
BIBLIOGRAPHY	30
APPENDIX A - HISTOGRAMS USED IN METHOD II MEASUREMENTS	33
APPENDIX B - UNCERTAINTY ESTIMATES	37
APPENDIX C - TABLES	39
APPENDIX D - FIGURES AND ILLUSTRATIONS	49

LIST OF TABLES

Table	Page
I. Previous Investigations Related to the Bursting Process . . .	40
II. Polymer Viscosity Ratios	41
III. Flow Conditions (Uncertainties: 19:1 Odds)	42
IV. Flow Conditions (Uncertainties: 19:1 Odds)	43
V. Flow Data Used in Evaluating Bursting Measurements by Achia	44
VI. Flow Data Used in Evaluating Donohue Et Al. Bursting Measurements	45
VII. Bursting Measurement Method I	46
VIII. Bursting Measurement Method II	47
IX. Downstream Viewing Lengths Used in Dye Visualization Experiments	48

LIST OF FIGURES

Figure	Page
1. Histogram of Ejection Rate/Unit Area as a Function of Downstream Distance for Water Flow, $U_{\tau} = 0.02078$ m/s, $M = 11.2$	34
2. Histogram of Ejection Rate/Unit Area as a Function of Downstream Distance for Drag Reducing Flow, 33% D.R., $M = 10$	35
3. Histogram of Ejection Rate/Unit Area as a Function of Downstream Distance for Drag Reducing Flow, 39.7% D.R., $M = 10$	36
4. Schematic of Two-Dimensional Channel and Circulation System .	50
5. End View of Flow Channel Illustrating Mirror and Lighting Arrangement Used in Experiments	51
6. Side View of Flow Channel Illustrating Maximum Lighting Angle With Channel Wall to Achieve Minimum Glare in Picture	52
7. Histogram of Ejection Rate/Unit Area as a Function of Distance Downstream of Dye Slot for Drag Reducing Flow at $M = 150$	53
8. Histogram of Ejection Rate/Unit Area as a Function of Distance Downstream of Dye Slot for Drag Reducing Flow at $M = 28.8$	54
9. Histogram of Ejection Rate/Unit Area as a Function of Distance Downstream of Dye Slot for Drag Reducing Flow at $M = 12$	55
10. Histogram of Ejection Rate/Unit Area as a Function of Distance Downstream of Dye Slot for Drag Reducing Flow at $M = 9$	56
11. Histogram of Ejection Rate/Unit Area as a Function of Distance Downstream of Dye Slot for Water Flow at $M = 21.7$	57

Figure	Page
12. Histogram of Ejection Rate/Unit Area as a Function of Distance Downstream of Dye Slot for Water Flow at $M = 9.9$	58
13. Bursting Period Measurements Made in Water at the Oklahoma State University Experimental Facility	59
14. Bursting Periods in Newtonian Flows Normalized With Inner Flow Variables, U_τ and ν	60
15. Bursting Periods in Newtonian Flows Normalized With Outer Flow Variables, U_ℓ and δ^*	61
16. Bursting Periods in Newtonian Flows Normalized With Outer Flow Variables, U_ℓ and δ	62
17. Bursting Periods in Drag Reducing Flows Normalized With Outer Flow Variables, U_ℓ and $D/2$	63
18. Present Bursting Period Measurements as a Function of the Amount of Drag Reduction Occurring in the Flow	64
19. Bursting Duration Normalized With Outer Flow Variables	65
20. Ratio of Bursting Duration to Bursting Period	66
21. Ratio of Polymer and Solvent Bursting Periods for Measurement Method I as a Function of Drag Reduction	67
22. Ratio of Polymer and Solvent Bursting Periods for Measurement Method II as a Function of Drag Reduction	68

NOMENCLATURE

A_c	cross sectional area of flow channel
D	pipe diameter or channel width
D_h	hydraulic diameter of flow channel, $4A_c/WP$
d_s	dye slot length transverse to flow direction
%D.R.	percent drag reduction, at constant velocity
F	spatially averaged bursting rate, burst count/(time x d_s)
M	ratio of the mass flow rate through the sublayer to mass flow rate through the dye slot, \dot{m}_s/\dot{m}_d
\dot{m}_s	mass flow rate through the sublayer, $\dot{m}_s = d_s \rho \int_{y=0}^{y=8\nu/u_\tau} u dy = 32d_s \rho \nu$
\dot{m}_d	mass flow rate through the dye slot
\dot{N}	number of events counted/sec
\dot{N}_e	number of ejections/cm ² sec
P	static pressure
Re_θ	Reynolds number based on momentum thickness, $U_\theta \theta/\nu$
T	temperature, °C
T_1	initial time of a bursting event disturbing a point near the wall
T_2	final time of a bursting event disturbing a point near the wall
T_b	time between bursting events, sec/burst
T_d	bursting duration at a point, sec
T_e	time between ejections, sec/ejection
U_{AVG}	mass averaged velocity
U_θ	centerline average velocity

U_τ	wall shear velocity $(\tau_w/\rho)^{1/2}$
u	velocity fluctuation component in the flow direction
v	velocity fluctuation component in the direction normal to the wall
WP	wetted perimeter
x^+	nondimensional coordinate in the streamwise direction, XU_τ/ν
y^+	nondimensional coordinate normal to the flow channel wall, YU_τ/ν

Greek Letters

Δ	difference
λ	average spacing between two adjacent low-speed streaks
λ^+	nondimensional streak spacing, $\lambda u_\tau/\nu$
ρ	density of the fluid
θ	momentum thickness
δ	boundary layer thickness
δ^*	displacement thickness

Subscripts

P	drag reducing flow
S	solvent flow

GLOSSARY OF SPECIAL TERMS

A glossary of special terms used throughout the text is provided at this point to make clear the discussion of physical processes. The meaning of some terms are self-explanatory. This glossary does not include definitions of commonly accepted terms used in turbulent flows. These definitions are designed with respect to dye visualization of fluid motions.

Wall Layer Structure. The distinct and quasi-regular flow structure found in the near-wall region of bounded shear layers. This consists of alternating regions in the transverse direction of low- and high-speed streaks.

Low-Speed Streak. A long, narrow, low-speed region of fluid in the near-wall region. Marking mediums tend to collect in these regions.

Ejection. A single filament of dye which is ejected from the near-wall region.

Bursting. Bursting consists of an overall process in which:

1. The low-speed streak is lifted up away from the wall.
2. The lifted streak undergoes an oscillatory growth motion.
3. A chaotic breakup of the streak in which one or more filaments are ejected.

The bursting process is continual in nature and is only separated into three parts for descriptive purposes only. The fact that bursts from a streak are observed as groups of spatially and temporally separated filaments reaffirms the hypothesis that distinct elements of

marked fluid are parts of one overall fluid motion. It is the overall process of these filaments ejecting themselves out into the flow that is used in this study to define a burst.

Sweep. A relatively large fluid eddy that has a streamwise velocity component greater than the local mean velocity, and that is moving toward the wall.

CHAPTER I

INTRODUCTION

Turbulent drag reduction by the addition of small amounts of long chain polymer molecules is defined as the reduction in viscous friction below that observed in an equal solvent flow.

This phenomenon has important engineering applications. For example, polymers have been added to water to increase the capacity of storm sewer systems during peak flow rates and to reduce power consumption in high pressure, high friction flows encountered in the servicing of oil fields. The drag reduction principle has application wherever frictional drag is a problem in liquid flows. Despite these successful applications, the phenomenon is not well understood and consequently, its potential may not have been fully exploited. The basic purpose of this thesis is to gain a better basic understanding of how the polymers affect the flow process.

The portion of the flow that needs to be studied is the wall region, because drag reduction is a wall phenomenon. As Wells and Spangler (28) seeped polymer into the wall layer through a slot in the wall of a pipe flow, they observed drag reduction just downstream of the slot. When they injected polymer along the centerline, drag reduction did not occur until the polymer had diffused to the wall from the center of the flow. This demonstrated that drag reduction is a phenomenon which occurs only when polymer is near the wall.

Drag reduction is a phenomenon which also occurs only when the flow is turbulent. A major feature of turbulent wall flows is the turbulent wall structure. This structure has been observed by many investigators. Kline et al. (13) reported the effect of the wall on the viscous sub-layer when they observed semi-coherent variations in the spanwise velocity. These variations were intermittent high-speed and low-speed regions. In visualization studies, the marking medium collects into the low-speed regions and forms long streaks. These streaks were first reported by Runstadler et al. (24). Visual investigations which have observed these streaks and measured their spacing in Newtonian flows include those of Donohue et al. (5), Oldaker (20), and Achia (1). Fortuna and Hanratty (6) measured the spacing of these streaks using an electro-chemical technique. Gupta et al. (10) formed autocorrelations from the velocity measurements of an array of hot wire sensors. The spacing of the resulting peaks in the short time averaged autocorrelations was an indication of a coherent structure existing in the sublayer. The results of all these techniques have confirmed that the nondimensional spacing of these streaks, λ^+ , is approximately 100 in solvent flows.

Kline et al. (13) reported that these streaks tend to drift slowly outward away from the wall. When the streak reaches a y^+ of approximately 12, it begins to oscillate. This oscillation amplifies itself and terminates in the abrupt breakup of the oscillating streak, with most of the breakups occurring in the buffer region, $10 < y^+ < 30$. Kline et al. (13) proposed that the time between bursts of a streak can be calculated from $T_b = 1/F\lambda$. Here F is the number of bursts counted/(time $\times d_s$), or \dot{N}/d_s . Donohue et al. (5) as well as Achia (1) have measured the bursting period in water flows using this equation for bursting

period. Kim et al. (11) visually measured the bursting period of water flows using a horizontal hydrogen bubble wire and also autocorrelations from hot wire measurements. Bursting periods from conditionally sampled hot wire measurements have been measured by Lu and Willmarth (16).

Offen and Kline (19) have recently measured the bursting period in water using an experimental method similar to the method used by Kim et al. (11). The difference in Offen and Kline's measurements was that they required bursts to be spatially separated from each other.* This is a new conceptual addition to the definition of a burst. Offen observed that a single burst could be composed of several ejections of fluid.

Kim et al. (11), Lu and Willmarth (16), and Wallace et al. (27) have shown that 70% of the total $|\rho u v|$ Reynold's stress is produced by the bursting process. This is 70% of the total production of turbulent kinetic energy. This production is also visually verified by the violence of the bursting process.

There are also other important production processes. Corino and Brodkey (3), Lu and Willmarth (16), Nychas et al. (18), and Wallace et al. (27) have observed sweeps of fluid traveling toward the wall at a velocity greater than the local mean. These "sweeps" are also major contributors to the total production of turbulent kinetic energy. Offen and Kline (19) observed an interaction between fluid from former bursts and the flow in the logarithmic region which results in sweeps. These new sweeps were observed to influence bursting further downstream.

*See bursting definition in "Glossary of Special Terms."

The universality of this structure was observed by Grass (9). He reported that bursts and sweeps are present in all bounded flows, independent of surface roughness. Gordon (8) has reported intermittent periods of high momentum transport in natural marine boundary layers as manifestations of the bursting process on a geophysical scale.

The overall picture these results present is a cycle of events in the wall region. Fluid collects into low-speed streaks, the streaks migrate away from the wall, the streaks become unsteady, begin to oscillate, and burst away from the wall, the bursts interact with fluid in the logarithmic region causing more sweeps, and the new sweeps return to the wall. These results focus the emphasis of this study of drag reducing flows toward the wall structure.

Streak spacing in drag reducing flows has been measured by Fortuna and Hanratty (6), Donohue et al. (5), Oldaker (20), and Achia (1). Fortuna and Hanratty (6) made their streak spacing measurements using an electro-chemical technique. The measurements of Donohue et al. (5), Oldaker (20), and Achia (1) were visual. A conflict existed between the measurements of Donohue et al. (5) and those of Fortuna and Hanratty (6). However, the recent measurements of Oldaker (20) and the measurements of Achia (1) have explained the differences in these earlier measurements.

Bursting period measurements in drag reducing flows have been made by Donohue et al. (5) and Achia (1). Both of these investigations used the relation for bursting period developed by Kline et al. (13), that $T_b = d_s / \dot{N} \lambda$. But while the author was assisting Oldaker (20) with his streak spacing experiments, it was observed that all the streaks marked at the dye slot were not bursting in the camera's field of view. To

count all bursts from streaks marked at the dye slot, the observer needed to see a much larger downstream distance than for water flows. Bursts from all streaks marked at the dye slot must be included in the total burst count to properly make the $T_b = d_s / \dot{N} \lambda$ measurement. This observation prompted the need for this series of experiments, as there was a question as to whether the measurements of Donohue et al. and the measurements of Achia were properly made.

A table which summarizes the previous bursting investigators and the type of measurements which each has made is provided in Table I, Appendix C.

Objectives

The objectives of this study were:

1. Develop a flow visualization technique capable of measuring the bursting period of turbulent channel flows. The flow visualization technique used marked fluid motions with dye which seeped into the flow through a slot in the channel wall.
2. Make measurements of this bursting period in solvent and drag reducing flows. The bursting periods, obtained in this study by two methods of measurement in both drag reducing flows and solvent flows, are reported in Chapter III and discussed in Chapter IV.
3. Observe how these measurements correlate with previous measurements which have been made. Discussion on how bursting periods measured in this study correlate with previous measurements, when scaled with inner and outer flow variables, and by themselves, appears in Chapter IV.
4. Observe structural changes in the drag reducing flows as they relate to the bursting process. Structural changes during the bursting

process are reported and discussed in Chapter IV.

From side-view motion pictures of dye motions, two types of measurements will potentially yield the bursting period of the flow. Conceptually, these two methods are:

1. Method I is based on counting all the bursting events from streaks which are marked very near the dye slot. Practically, one must have a field of view which is long enough in the streamwise direction that one can see all of these streaks burst. Then $T_b = d_s / \dot{N} \lambda$. This type of measurement is physically the bursting period of a streak.

2. Method II yields the bursting period in a small incremental area of the flow. In this method, there must be sufficient dye at that small area to mark all the bursting events which occur. In this case, discrete samples of T_b are obtained from the temporal record of the occurrence of bursts.

The essential differences of the two methods are the extent of the field of view in the downstream direction and the criteria for choosing these fields of view. In method I, the field of view is large because one must count all bursts from streaks marked at the dye slot. In method II, the field of view is small but the location must be chosen so as to ensure that all the events which are occurring are marked by the dye. In both methods, the spanwise dye slot length should be less than or equal to λ , so that the probability of one burst obscuring another burst is minimized.

CHAPTER II

EXPERIMENTAL PROCEDURE

In this study, a fluorescent orange dye was used to mark the fluid motions near the wall and therefore measure the bursting period in turbulent channel flows. Moderate speed motion pictures were taken of the dye motions. The fluorescent dye provided excellent filming contrast between the bursting events and the surrounding background fluid motions. The fluids used in these experiments were dilute polymer solutions and tap water. A procedure for counting bursts was developed which successfully discriminated between bursts and ejections of fluid away from the wall.

Experimental Apparatus

These experiments were conducted in the Basic Fluid Dynamics Laboratory, School of Mechanical and Aerospace Engineering, Oklahoma State University, Stillwater, Oklahoma. The flow system used in these experiments is shown in Figure 4. The flow channel was constructed by Donohue et al. (5) and modified by Oldaker (20). The flow system was constructed by Reischman (23).

The flow channel is nominally 38 mm wide, 454 mm tall, and 2.54 m long. The flow cross sectional area is 175.82 cm^2 and the hydraulic diameter is 71.67 mm. The upstream settling chamber is equipped with two screens to redistribute the flow evenly across the cross section,

and the entrance to the channel is rounded. The flow in the channel is two-dimensional. The channel is equipped with two 0.127 mm dye slots milled into the wall 44 and 51 channel widths downstream of the entrance. The system is equipped with three Matheson rotometers capable of measuring dye flow rates through the slot from 0.001 ml/s to 3 ml/s. The channel is equipped with two 3.175 mm diameter pressure taps. The first tap is 46.8 channel widths downstream of the entrance. The second tap is an additional 12 channel widths downstream. A more detailed description of this flow facility is available in Oldaker (20).

Experiments were conducted in this flow facility using both dilute polymer solutions and tap water. The centrifugal pump shown in Figure 4 was not used as neither the polymer nor the water were reused or recirculated. This procedure kept mechanical degradation of the polymer to an absolute minimum and maintained good clarity for photography purposes. The solutions were collected in the 13.63 m³ tank and then blown through the flow system. The entire flow facility has been constructed of acrylic, PVC, and stainless steel to minimize contamination from the system itself.

Polymer Solutions

The interesting quality of the drag reduction phenomenon is that large drag reductions are possible at very low concentrations. Paterson and Abernathy (21) report drag reductions of around 15% with concentrations as low as 1 wppm and $Re_d = 12,000$. This type of solution is thermodynamically dilute, that is, the average distance between the polymer molecules is greater than the diameter of the molecules.

The polymer solutions used in this study were thermodynamically dilute. The polymers themselves were high molecular weight polyacrylamides. Their brand names were Separan AP 273, a product of the Dow Chemical Company, and Calgon TR0 323, a product of Calgon Corporation. Virk et al. (26) has pointed out that thermodynamically dilute solutions have viscosity ratios of approximately two. The viscosity ratio is the ratio of the viscosity of the solution to the viscosity of water at the solution temperature. Viscosity ratios for the solutions used here were measured at a shear rate of 73 sec^{-1} and are shown in Table II, Appendix C. The measurements were made using a Brookfield Model LV Synchro-Lectric Viscometer with UL adapter, O.S.U.-M.E. #351. By Virk's criterion, all the solutions can be classified as dilute.

Preparation of Polymer Solutions

The polymer solutions used in these experiments were prepared by first mixing a concentrated solution (1000 to 2000 wppm) and then diluting the concentrated solution to the desired concentration, 50 or 100 wppm.

The first step in the mixing process was heating the water in an open 0.38 m^3 stainless steel tank to approximately 30°C using an immersion heater. Either 681 grams or 1362 grams of polymer crystals were then added to approximately 3 liters of isopropanol and suspended in a slurry by continuous stirring. The mixing tank was stirred thoroughly, as quickly as possible, to prevent the forming of agglomerations or so-called "fish-eyes." This process was essential in obtaining a homogenous mixture. The polymer solutions were stirred occasionally during a minimum hydration period of 1.5 hours. After the hydration period, the

concentrated solution was diluted to the appropriate concentration. Dilution was accomplished by gently stirring the proper amount of polymer concentrate and water.

Drag Reduction

The reduction in frictional drag, which is observed in dilute polymer flows, is defined as the percent reduction in pressure drop, compared to the pressure drop of a solvent at the same flow rate. In symbols:

$$\text{Percent Drag Reduction} = \frac{\Delta P_S - \Delta P_P}{\Delta P_S} \times 100.$$

This is evaluated at $U_{\text{AVG}} = \text{constant}$ for polymer and solvent. The solvent viscosity is evaluated at the temperature of the polymer solution.

Channel Wall Shear Stress and Mass Averaged Velocity Measurements

The wall shear stress during each experiment was calculated from the pressure difference measured between two 3.18 mm diameter pressure taps located 83 mm above the bottom of the channel and spaced 12 channel widths apart. A two fluid micromanometer using carbon tetrachloride and water was used to measure the pressure difference between the two ports. The micromanometer dial was marked in 0.05 mm divisions and was capable of being read to 0.025 mm. Its pointer was a stainless steel needle milled on a lathe to a very sharp point. Pressure drop equilibrium was obtained before and after each measurement.

Accurate flow rates were obtained by timing a measured volume of fluid caught in a 0.152 m^3 rectangular stainless steel bucket. The bucket was mounted on wheels and placed in the 2.27 m^3 open top catch

tank. It could then be quickly rolled under the weir tank for filling and be quickly removed when full. The collection time was obtained through the use of a stop clock and was accurate to 0.2 seconds, which included the reaction time of the observer watching the bucket. The mass averaged velocity was calculated from the flow rate measurements. The wall shear stress was obtained from the pressure drop measurements, using a force balance on a bounded control volume of fluid.

Flow Visualization

The flow visualization techniques used in this study are similar to techniques used by Oldaker (20). A 0.12% solution of water soluble Rhodamine B Base, available through the Eastman Kodak Company, was used as the means of marking the flow. The dye was chosen because of its brilliant fluorescent orange color when it is observed at 90° to its lighting source. This dye mixed well with polymer as well as water.

The brilliant orange color produced by the Rhodamine B dye when it fluoresces is needed to achieve good contrast in the motion pictures. This means that all unnecessary glare must be eliminated. The lighting required is similar to that required by hydrogen bubble experiments. The lighting technique which worked the best was a high intensity light source, in our case, a 600 watt overhead projector, pointing at a very shallow angle with the flow channel wall (see Figures 5 and 6). An angle greater than 45° significantly increased the glare in the picture.

The flow was viewed through the top of the channel by means of a single front surface mirror. The mirror was tilted at 45° for ease of viewing (see Figure 5).

Movies were filmed of the flow as events occurred too fast to analyze them as they occurred. Initially, movies were filmed with Kodak 4-X Super 8 black and white film in a Beaulieu 4008 Zm II Super 8 movie camera and analyzed with a Kodak Ektagraphic MSF-8 projector. During the analysis of the initial experiment this projector suffered a mechanical failure. Since a replacement projector was not available, there was a change to 16 mm film because better film analysis facilities were available. The remainder of the films used were 16 mm Kodak 4-X black and white film and were taken with a Bolex H16 movie camera. The 16 mm movies were analyzed frame by frame using a Bell and Howell time and motion projector. All movies were filmed with either a 75 mm f1.9 lens or a 75 mm f1.4 lens.

Data Reduction

Each technique for measuring the characteristic period of a burst required a different technique for data reduction.

Measurement Method I

To correctly make measurement method I, it was necessary to simultaneously see both the side and top views of the flow to be certain that only bursts from streaks marked at the dye slot were counted, and that all the streaks marked at the dye slot burst in the field of view. The fluorescent dye used in these experiments only allowed a top view due to tremendous glare problems on the channel wall. To make sure that all bursts were observed, filming was done over several 12.75 cm segments downstream of the dye slot. This procedure was repeated so that the entire length of the potential viewing area downstream of the dye slot,

45 cm, was analyzed for drag reducing flows. Only one segment was necessary in water flows. As a test to check the possibility of one burst being obscured by previous upstream bursts, film records were made at equal flow conditions for $d_s = \lambda$, and $d_s = \lambda/9$. The shorter dye slot significantly reduced all background clutter due to dye filaments from previous bursts. The total number of bursts in the entire viewing field was counted to determine \dot{N} as the films were viewed in reverse motion. This type of viewing permitted accurate determination of the bursting origin. $T_b = d_s / \dot{N} \lambda$ was then calculated.

Measurement Method II

As previously discussed, method II required that sufficient dye was present at the measurement point to mark all of the events which were occurring at that point. Consequently, some experiments were conducted to show that it is feasible to get sufficient dye into the wall layer. These are described in Chapter III, "Test to Demonstrate Feasibility of Method II." As in method I, the movies were viewed in reverse to obtain accurate bursting origins.

While viewing these films, it was observed that the bursting event occurs over a period of time rather than at a specific instant. To account for this "active" period, a time T_1 was recorded when the measurement point was first disturbed by an ejection from the burst returning to the wall. A time T_2 was recorded when the last ejection of the burst disturbed the measurement point. An average time $(T_1 + T_2)/2$ was used as a reference time to compare with the previous burst's reference time. The difference between these two reference times is, by definition,

the bursting period. An ejection disturbance within ± 0.6 cm from the measurement point was considered a disturbance at the point.

CHAPTER III

EXPERIMENTAL RESULTS

Test to Demonstrate Feasibility of Method II

The desire to know the area of the flow where there was sufficient dye to mark all the events that are occurring in a small area motivated an experiment where the dye flow rate was varied, the flow conditions remained constant, and the ejection rate per unit area was measured from the motion picture records as a function of downstream distance. The hypothesis for this experiment was that there would be a region where ejection rate per unit area would be constant, independent of dye flow rate, if sufficient dye was in the flow. This region would move forward with increased flow rate of dye.

The experimental apparatus was modified such that the total field of view was now approximately 56 cm downstream of the dye slot. The experiment to determine where sufficient dye was present was conducted with 50 wppm AP 273 at 17.25% drag reduction. The experiment was designed to vary the dye flow parameter, M^* , with values of $M = 150, 28.8, 12, 9, \text{ and } 6$. The result desired from the set of experiments was the downstream location, with respect to the dye slot, where the ejection rate per unit area was constant.

* See definition of M in "Nomenclature."

Histograms which resulted from these measurements, when $9 \leq M \leq 150$, are presented in Figures 7 through 10. The fact that the maximum magnitude is essentially constant at $\dot{N}_e = 3.5 \pm 0.5$, for values of $M = 28.8$, 12, and 9, demonstrates that there is sufficient dye in these plateau regions. One factor which could account for the variance of the magnitudes in the plateau regions was that the maximum analysis time for an increment was approximately 40 seconds. Fifteen to twenty ejections were counted during this period in each increment of the plateau. It is believed that this number of samples is only sufficient to show the trend in the data and a large spread in the data can be expected. Another factor which accounts for some variance in magnitude was that ejections counted in the farthest right increment of each film segment were always less in number than the ejection counts obtained from the rest of the increments in the film segment. Each increment was 2.54 cm wide and each segment consisted of four or five increments. It was very difficult to observe an ejection without a path to follow to the surface of the wall. The area used to normalize the number of ejections counted in each segment was the product of the downstream observation increment and the transverse length of the dye slot.

The histograms illustrate the movement of the constant magnitude area forward with increased dye flow rate. For a value of $M = 150$, the plateau was never reached. There simply was not sufficient dye to mark all the events in the near-wall layer. At a value of $M = 6$, the near-wall layer was observed to be disturbed by the dye flow rate itself. It was essentially flooded with dye from the dye slot.

Histograms for water flows are shown in Figures 11 and 12. The histograms take the same form as those of the drag reducing flow, except

they rise faster, have a shorter plateau, and then drop off more quickly.

Bursting Period Measurements

Water Flows

Measurement Method I. With $d_s = \lambda$, measurement method I essentially measures the bursting period of a streak. The bursting measurements made using method I are recorded in Table VII, Appendix C. These results indicate that the bursting event size is of order λ . Two dye slot widths were used to determine the possibility of a streak's burst being obscured by a previous burst. By reducing the dye slot width from λ to $\lambda/9$, background noise from previous bursts was substantially reduced. Without the noise, the initial and final portions of a burst were more definable. Comparing burst counts from two similar water flows, wall shear velocities of 0.02078 m/s and 0.02048 m/s, the burst counts were approximately the same for λ and $\lambda/9$ dye slot lengths. The burst counts for water flows at wall shear velocities of 0.0173 m/s and 0.01725 m/s are different for the two slot lengths, but the observation times are also different. The net result is that the bursts per unit time is about the same. Since the two slot lengths yield approximately the same bursting rates both must have the same capability of marking a burst. Therefore, bursting events must be relatively large size events, of order λ .

The method I, $T_b = d_s / \dot{N} \lambda$, bursting period measurements at $d_s = \lambda/9$ disagree with those obtained for essentially equal flow conditions at $d_s = \lambda$ (see Figure 13). However, as the bursting event size is on the order of λ , it would be more appropriate to use $d_s = \lambda$ in the bursting

period equation, even when d_s is much less than λ . With this substitution, the periods calculated for the same flow conditions using both slot widths are the same order of magnitude. Figure 13 suggests that present method I measurements extend the trend established by bursting measurements of Donohue et al. (5). However, a much better comparison with other data can be made on nondimensional plots.

In this thesis, nondimensional bursting periods are plotted as a function of Re_θ so that the boundary layer data may be included on the figures. For channel flows, momentum thickness, θ , and displacement thickness, δ^* , were obtained using a computer model developed by Reischman (23), which predicted the entire mean velocity profile. This computer model uses the Cess (2) model for turbulent diffusivity. The predictions are based upon knowledge of U_τ , U_{AVG} , and ν . Reischman tested the model for seven drag reducing flows with three different polymer types and a range of drag reductions of 24% to 40%. Over this range of parameters, the model does an excellent job of predicting the mean velocity profile.

In pipe flows, a computer program developed by Ghajar (7) was used to predict the velocity profiles of the flow. The program used the Cess (2) model for turbulent diffusivity, and exactly predicted velocity measurements made by Virk et al. (26).

The assumption was made that the boundary layer at the observation point was fully developed and that $\delta =$ one half the channel width or pipe width. The predicted velocity profiles were numerically integrated to obtain the displacement thickness and the momentum thickness, where at constant density:

$$\delta^* = \int_{y=0}^{y=\delta} \left(1 - \frac{U}{U_{\zeta}}\right) dy$$

$$\theta = \int_{y=0}^{y=\delta} \frac{U}{U_{\zeta}} \left(1 - \frac{U}{U_{\zeta}}\right) dy$$

The bursting periods are normalized and plotted nondimensionally, so that they may be compared to other investigator's measurements as well as to observe which variables form a nondimensional bursting period, independent of Re_{θ} . In Figure 14, the bursting periods are normalized with inner flow variables, u_{τ} and v . The method I points lie close to the line proposed from data correlated by Rao et al. (22), which is a direct function of Re_{θ} . This was the most critical test of the bursting period measurements, as only one predicted parameter, θ , was involved in the plot. The water data does not scale independent of Re_{θ} ; therefore, other normalizing variables were used.

The method I bursting periods are normalized with two sets of outer flow variables, (U_{ζ}, δ^*) and (U_{ζ}, δ) , in Figures 15 and 16. The bulk of the data normalized with U_{ζ} and δ^* is independent of Re_{θ} in Figure 15. The data normalized with U_{ζ} and δ in Figure 16 is slightly dependent on Re_{θ} . As δ is represented by $D/2$ in channel and pipe flows, (U_{ζ}, δ) are the normalizing variables used in the remainder of this study. In each figure, periods measured at Re_{θ} less than 500 tend to rise steeply with decreasing Re_{θ} . This behavior might be expected as the flow approaches transition to laminar flow.

Measurement Method II. This method physically measures the bursting period at a very small area in the flow. It is based on the decision that sufficient dye is available at the measurement point to mark all the events which occur. The availability of a sufficient amount of dye was

based on the existence of a plateau region of the $\dot{N}_e^+(x^+)$ histograms. Histograms for the remainder of the flows analyzed in this study are available in Appendix A.

Method II bursting measurements also show that the bursting event size is of order λ . This was confirmed by checking the burst counts for two essentially equal water flows, but two different values of d_s . At 0.02078 m/s and 0.02048 m/s, as well as 0.0173 m/s and 0.01725 m/s, the burst counts at $d_s = \lambda$ and $d_s = \lambda/9$ are very similar. These values are available in Table VIII, Appendix C.

The water values obtained through the method II technique are compared to other water bursting periods measured in this experimental facility in Figure 13. They are definitely higher values than previously measured bursting periods, including those deduced in this study using the method I technique. This is an expected result as the burst counts were taken over a much smaller area than used in the method I measurements. These method II bursting periods are normalized with outer flow variables and plotted in Figures 15 and 16.

Method II periods are higher, when compared to previously measured bursting periods. The hydrogen bubble time line measurements of Offen and Kline (19) were probably taken over an area of length similar to the plateau region of the water histograms in Figures 11 and 12. Their burst count would be similar to the count obtained in method I, not method II.

Hot wire measurements, similar to those by Rao et al. (22) or Lu and Wilmarth (16) are not point measurements. The hot wire probe, situated at possibly $y^+ = 15$, is sensitive to fluid events that originate upstream of the measuring point. This upstream distance or "coherence

length" of the flow, is unknown. If it were approximately equal to the plateau region of the water histograms of Figures 11 and 12, the hot wire results would be expected to be similar to method I measurements, and they would not be expected to agree with method II measurements, which were made over a much smaller area.

When normalized with inner flow variables in Figure 14, the method II periods are higher than the periods measured with method I or with hot wire probes.

Drag Reducing Flows

All of the present bursting period measurements that have been made in drag reducing flows are presented in Figure 17. The bursting periods are nondimensionalized using outer flow variables, U_∞ and $D/2$.

Measurement Method I. The normalized bursting periods of a streak from present measurements continue the trend initiated by measurements of Donohue et al. (5) and Achia (1). A much longer observation distance was used in this study, than was used in the experiments of Achia (1) or Donohue et al. (5). These downstream distances are noted in Table IX, Appendix C. The drag reduction occurring in each of the studies was similar. In the present study, a definite distinction between bursts and ejections was made.

Agreement between measurement method I and measurements by Donohue et al. (5) is reasonable because Donohue used a high dye flow rate, and the major part of the plateau region was probably included in his counting area. Also, when an unbiased observer is asked to count bursts, and no discrimination between bursts and ejections is used, bursts, not ejections, are usually counted. Donohue did not make a direct

distinction between bursts and ejections. The spread between Donohue's data and the points obtained from method I may be sufficiently small to go unnoticed on Figure 17. Insufficient information is available about the counting method used by Achia to comment on his measurements.

The bursting counts obtained for method I measurements in drag reducing flows reaffirm the idea that the bursting event size is on the order of λ . These counts may be obtained in Table VII, Appendix C. For values of $d_s = \lambda$ and $d_s = \lambda/9$, the burst counts are essentially equal in experiment set R-11.

Insufficient statistical data is available to observe how nondimensional method I bursting periods scale with drag reduction. Two experimental data points are plotted in Figure 18.

Measurement Method II. This measurement is the bursting period at a small area in the flow. From Figure 17, these values of T_b in drag reducing flows increase as Re_θ increases. This nondimensional bursting period does not scale on drag reduction, as observed in Figure 18.

Bursting Period Durations

With measurement method II it is possible to simultaneously measure the duration of a burst in the measurement area, as well as the bursting period. The duration of the bursting event is longer in drag reducing flows than in solvent flows. T_d , the duration of a burst, was normalized with outer flow variables and plotted in Figure 19. The present measurements reflect the trend of bursting data reported by Lu and Willmarth (16). Although the hot wire measurements were taken over a much different area than method II, the bursting duration is still statistically

comparable to method II measurements of T_d . This is because the bursting duration from any population of data should be comparable to the duration from any other.

CHAPTER IV

DISCUSSION

The objectives of this study were to:

1. Develop a flow visualization technique capable of measuring the bursting period of turbulent channel flow.
2. Make the measurements of the bursting period in solvent and drag reducing flows.
3. Observe how these measurements correlate with previous measurements which have been made.
4. Observe structural changes in the drag reducing flows as they relate to the bursting process.

Measurement Technique

This study has observed three types of bursting period measurements. Each is essentially different.

Measurement method I evaluates the bursting period of streaks marked at the dye slot, with $d_s = \lambda$. With $d_s = \lambda/9$, the total burst count is very similar to the count obtained with $d_s = \lambda$. This suggests that the bursting event size is of order λ . When d_s is less than λ , a more meaningful result is obtained by evaluating the bursting period of a streak with $d_s = \lambda$ rather than the shorter d_s used in the experiment. The smaller dye marker could miss a few events, but this substitution yields a more meaningful number because the size of the bursting events

is of order λ and therefore they are usually detected with all dye slots where d_s is less than or equal to λ .

The measurements made using method II are measurements of the bursting period at a very small area in the flow. In this technique, only dye filaments affecting the immediate area surrounding the measurement point are included in the burst count. With this technique, the direct burst counts are unbiased by any other parameter in obtaining the bursting period. This type of measurement has direct application in current surface renewal models.

The conditionally sampled hot wire measurements, with which present measurements are compared, are bursting periods measured over the coherence length of the flow upstream of the hot wire probe. In Newtonian flows, the conditionally sampled hot wire burst counts could be expected to agree with method I burst counts, as they could be made over approximately the same measurement area.

Bursting Period Correlations

The object of correlating bursting periods with different sets of variables is to determine which variables independently control the bursting period. The bulk of the data indicates that (U_C, δ^*) , and to a large extent (U_C, δ) , form a constant, nondimensional period, independent of Re_θ , for Newtonian flows. The most useable nondimensional period presented in this study is $T^+ = \frac{T_b U_C}{D/2}$. This is observed in Figure 16 for Newtonian flows and Figure 17 for drag reducing flows. The period is slightly dependent upon Re_θ for Newtonian flows measured by method I and conditionally sampled hot wire measurements. For pipe and for channel flows, the period involves one less calculation, as $D/2$

is the pipe radius or one half the channel width. Only a rough estimate of Re_θ is required to predict the bursting period. The bursting periods of Kim et al. (11) yield $T^+ = 6.3$ at $Re_\theta = 666$ and $T^+ = 4.6$ at $Re_\theta = 1100$. The periods agree with present hot wire, present method I, and hydrogen bubble bursting period measurements. Although Kim did not place the requirement of spatially separation on his burst data, he must have used this criterion while actually making his burst counts. Motion pictures filmed during experiments of Donohue et al. (5) suggest that bursts, rather than single ejections, were counted in his data. Donohue's normalized bursting periods are located in a region of Re_θ very close to transition to laminar flow. In this region, T^+ appears to rise steeply with increasing Re_θ .

All previous dye visualization bursting periods have been obtained with $d_s = \lambda$. At high values of Re_θ , a tremendous amount of kinetic energy production occurs in the marked regions of the flow. With $d_s = \lambda$, it is very difficult to make a definite distinction between bursting events. This may account for the tremendous spread in the bursting periods of water flows presented in Figures 14, 15 and 16.

In Figure 17, it is observed that the additional downstream length as well as the definite distinction between bursts and ejections did not make a significant difference in the reported bursting period. Beyond an $x^+ = 2000$, bursts from the wall could have been obscured by lateral motion from previous bursts' filaments in the buffer region. From movies of Donohue's experiments, the majority of the plateau region was probably included in Donohue's counting area.

The bursting period at a small area in the flow, method II, is the type of measurement potentially useful in surface renewal models. In

each comparison, the T^+ formed from method II periods is a direct function of Re_θ . Therefore, an accurate prediction of Re_θ is necessary for an accurate prediction of T^+ (method II). This is observed in Figures 14 through 17.

The ratio of bursting duration to bursting period is shown in Figure 20. Conditionally sampled hot wire periods and the average bursting period of a streak are included in the figure.

Structural Changes Occurring in Drag Reducing Flows

With increasing drag reduction, the spacing of the streaks in the flow increases. There are fewer streaks; therefore, fewer bursts. Method I measures the bursting period of a streak. If no structural changes were occurring, the ratio of T_b in polymer to T_b in water at an equal wall shear stress would be equal to one. The present data, as well as the bulk of the data from previous investigators, indicate an increasing ratio with increasing drag reduction (see Figure 21). The streaks are becoming more stable with increasing drag reduction.

The ratio of T_b in polymer and water for method II measurements is always greater than one (see Figure 22). The ratios at 16% D.R. and 33% D.R. were obtained with Calgon TR0 323 polymer. Separan AP 273 was the polymer used for the two points at approximately 40% D.R. The drop in the ratio at 40% D.R. is taken as an indication of polymer type rather than a structural change occurring in the flow. If a structural change were occurring in the 40% D.R. region, an indication of it would be expected on Figure 21.

CHAPTER V

CONCLUSIONS AND RECOMMENDATIONS

Based on the reported results and observations made in this study, the following conclusions and recommendations have been reached.

Conclusions

1. The average bursting period of a streak measured in this study agrees with the measurements of previous investigators in both solvent and drag reducing flows.
2. The bursting event size is of order λ .
3. When using $T_b = d_s / \dot{N}\lambda$ to obtain the average bursting period of a streak and d_s is less than λ , λ should be substituted for the actual value of d_s used in the experiment.
4. Sufficient dye is present in the flow near the wall to mark all the events which are occurring, when \dot{N}_e' becomes independent of distance downstream of the dye slot.
5. Present measurements of the bursting period at a small area in the flow increase with increasing Re_θ in drag reducing and solvent flows. This type of measurement has a direct application to surface renewal models.
6. Structural changes observed indicate that there is decreased bursting in drag reducing flows due to the increased spacing of the

streaks. All of the bursting measurements indicate that the streaks become more stable with increased drag reduction.

Recommendations

Based on the conclusions reached in this study, the following recommendations for further research are made:

1. Measurements of the bursting period in drag reducing flow are necessary using either a conditionally sampled hot wire probe system, or laser doppler anemometry. The conditionally sampled hot wire system would verify the bursting period of a streak, while the laser doppler anemometry system would make a bursting period measurement at a single point in the flow.

In further visual studies:

2. Perform a series of experiments using dye visualization and conditionally sample hot wire measurements to try and observe the size of the "coherence length" in solvent and drag reducing flows.

3. A series of experiments are necessary to determine the burst count dependence on d_s .

4. Extend the present dye visualization technique to higher drag reductions, and higher Re_θ in solvent flow.

5. Observe if an \dot{N}_b plateau is formed in the \dot{N}_e plateau region.

BIBLIOGRAPHY

- (1) Achia, B. U. "Structure of Pipe Wall Turbulence in Newtonian and Drag-Reducing Flow: A Hologram-Interferometric Study." (Ph.D. Thesis, The University of British Columbia, 1975.)
- (2) Cess, R. D. "A Survey of the Literature in Heat Transfer in Turbulent Tube Flow." Westinghouse Research Report 8-0529-R24. Philadelphia: Westinghouse Corp., 1958.
- (3) Corino, E. R., and R. S. Brodkey. "A Visual Investigation of the Wall Region in Turbulent Flow." Journal of Fluid Mechanics, Vol. 37 (1969), p. 1.
- (4) Donohue, G. L. "The Effect of a Dilute, Drag-Reducing Macromolecular Solution on the Turbulent Bursting Process." (Ph.D. Thesis, Oklahoma State University, 1972.)
- (5) Donohue, G. L., W. G. Tiederman, and M. M. Reischman. "Flow Visualization of the Near-Wall Region in a Drag-Reducing Channel Flow." Journal of Fluid Mechanics, Vol. 56, Pt. 3 (1972), pp. 559-575.
- (6) Fortuna, G. and T. J. Hanratty. "The Influence of Drag-Reducing Polymers on Turbulence in the Viscous Sublayer." Journal of Fluid Mechanics, Vol. 53 (1972), p. 575.
- (7) Ghajar, A. "Prediction of Heat Transfer Coefficients in Drag Reducing Turbulent Pipe Flows." (M.S. Thesis, to be submitted to the Graduate Faculty, Oklahoma State University, December, 1975.)
- (8) Gordon, C. M. "Period Between Bursts at High Reynolds Number." The Physics of Fluids, Vol. 18, No. 2 (February, 1975), pp. 141-143.
- (9) Grass, A. J. "Structural Features of Turbulent Flow Over Smooth and Rough Boundaries." Journal of Fluid Mechanics, Vol. 50, Pt. 2 (1971), pp. 233-255.
- (10) Gupta, A. K., J. Laufer, and R. E. Kaplan. "The Spatial Structure in the Viscous Sublayer." Journal of Fluid Mechanics, Vol. 50, Pt. 3 (1971), pp. 493-512.

- (11) Kim, H. T., S. J. Kline, and W. C. Reynolds. "An Experimental Study of Turbulence Production Near a Smooth Wall in a Boundary Layer With Zero Pressure Gradient." Report No. MD-20. Stanford, Calif.: Stanford University, Thermosciences Division, Department of Mechanical Engineering, 1968.
- (12) Kline, S. J. and F. A. McClintock. "Uncertainties in Single Sample Experiments." Mechanical Engineering, Vol. 75 (January, 1953), pp. 3-8.
- (13) Kline, S. J., W. C. Reynolds, F. A. Schraub, and P. W. Runstadler. "The Structure of Turbulent Boundary Layers." Journal of Fluid Mechanics, Vol. 30 (1967), pp. 741-773.
- (14) Laufer, J. and M. A. Badri Narayanan. "Mean Period of the Turbulence Production Mechanisms in a Boundary Layer." The Physics of Fluids, Vol. 14 (1971), pp. 182-183.
- (15) Lu, S. S. and W. W. Willmarth. "Measurement of the Mean Period Between Bursts." The Physics of Fluids, Vol. 16, No. 11 (November, 1973), pp. 2012-2013.
- (16) Lu, S. S. and W. W. Willmarth. "Measurements of the Structure of the Reynolds' Stress in a Turbulent Boundary Layer." Journal of Fluid Mechanics, Vol. 60, Pt. 3 (1973), pp. 481-511.
- (17) Meek, R. L. "Period Fluctuations Near the Wall in Turbulent Flows." AIChE Journal, Vol. 18, No. 4 (July, 1972), pp. 854-855.
- (18) Nychas, S. G., H. C. Hershey, and R. S. Brodkey. "A Visual Study of Turbulent Shear Flow." Journal of Fluid Mechanics, Vol. 61 (1973), p. 513.
- (19) Offen, G. and S. J. Kline. "Combined Dye-Streak Hydrogen-Bubble Visualization Observations of a Turbulent Boundary Layer." Journal of Fluid Mechanics, Vol. 62 (1974), p. 223.
- (20) Oldaker, D. K. "An Experimental Investigation of the Near-Wall Flow Structure During Drag Reduction." (M.S. Thesis, Oklahoma State University, 1974.)
- (21) Paterson, R. W. and F. H. Abernathy. "Transition to Turbulence in Pipe Flow for Water and Dilute Solutions of Polyethylene Oxide." Journal of Fluid Mechanics, Vol. 51 (1972), pp. 177-185.
- (22) Rao, K. N., R. Narasimha, and M. A. Badri Narayanan. "The Bursting Phenomenon in a Turbulent Boundary Layer." Journal of Fluid Mechanics, Vol. 48, Pt. 2 (1971), pp. 339-352.
- (23) Reischman, M. M. "Laser Anemometer Measurements in Drag Reducing Flows." (Ph.D. Thesis, Oklahoma State University, 1973.)

- (24) Runstadler, P. W., S. J. Kline, and W. C. Reynolds. "An Experimental Investigation of the Flow Structure of the Turbulent Boundary Layer." Report No. MD-8. Stanford, Calif.: Stanford University, Thermosciences Division, Department of Mechanical Engineering, 1963.
- (25) Schraub, F. A. and S. J. Kline. "A Study of the Turbulent Boundary Layer With and Without Longitudinal Pressure Gradients." Report No. MD-12. Stanford, Calif.: Stanford University, Thermosciences Division, Department of Mechanical Engineering, 1965.
- (26) Virk, P. S. et al. "The Toms Phenomenon: Turbulent Pipe Flow of Dilute Polymer Solutions." Journal of Fluid Mechanics, Vol. 30, Pt. 2 (1967), pp. 305-328.
- (27) Wallace, J. M., H. Eckelmann, and R. S. Brodkey. "The Wall Region in Turbulent Shear Flow." Journal of Fluid Mechanics, Vol. 54 (1972), p. 39.
- (28) Wells, C. S. and J. G. Spangler. "The Injection of a Drag Reducing Fluid Into Turbulent Pipe Flow of a Newtonian Fluid." The Physics of Fluids, Vol. 10, No. 9 (1967), p. 1890.

APPENDIX A

HISTOGRAMS USED IN METHOD II MEASUREMENTS

This appendix contains histograms used, in addition to those present in the figures, to determine that sufficient dye was present at the measuring point for accurate method II measurements.

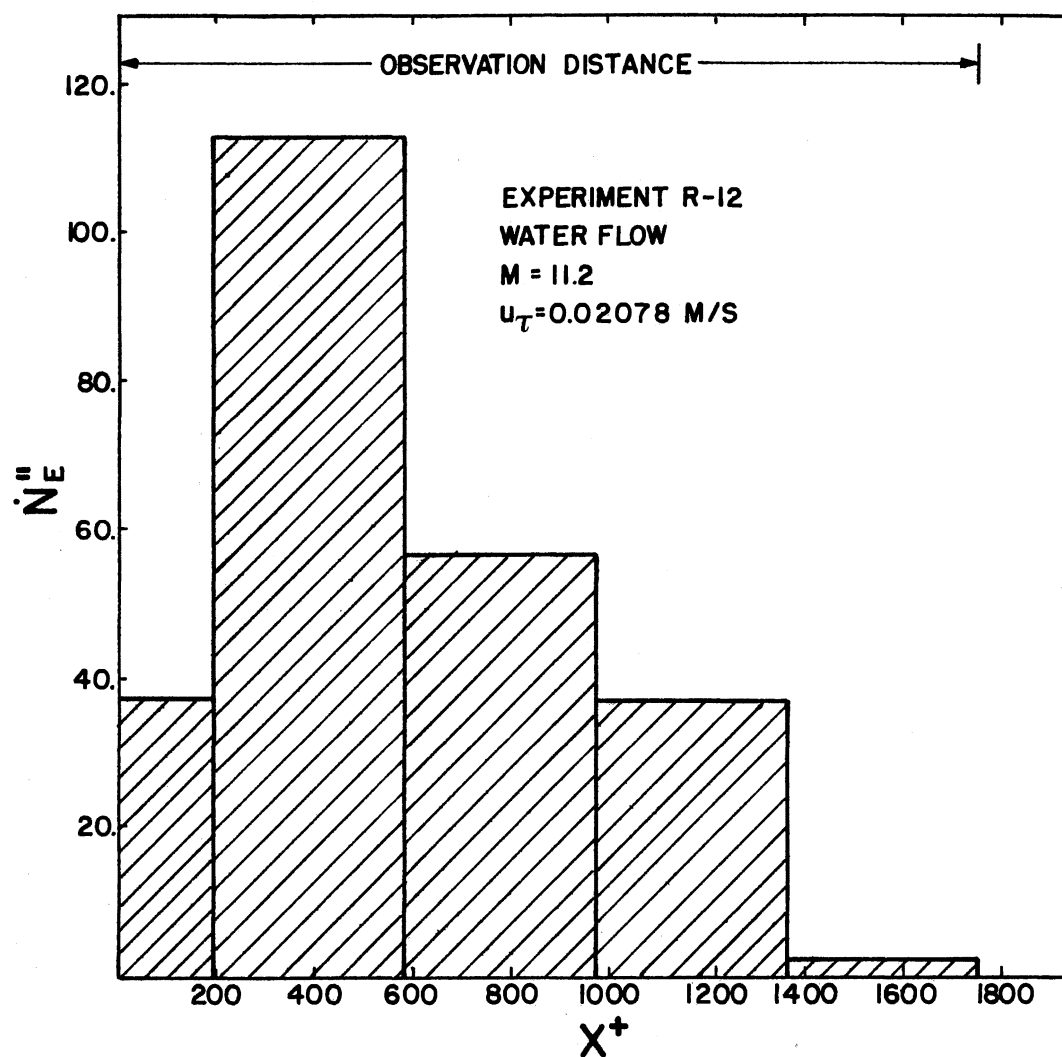


Figure 1. Histogram of Ejection Rate/Unit Area as a Function of Downstream Distance for Water Flow, $U_T = 0.02078 \text{ m/s}$, $M = 11.2$

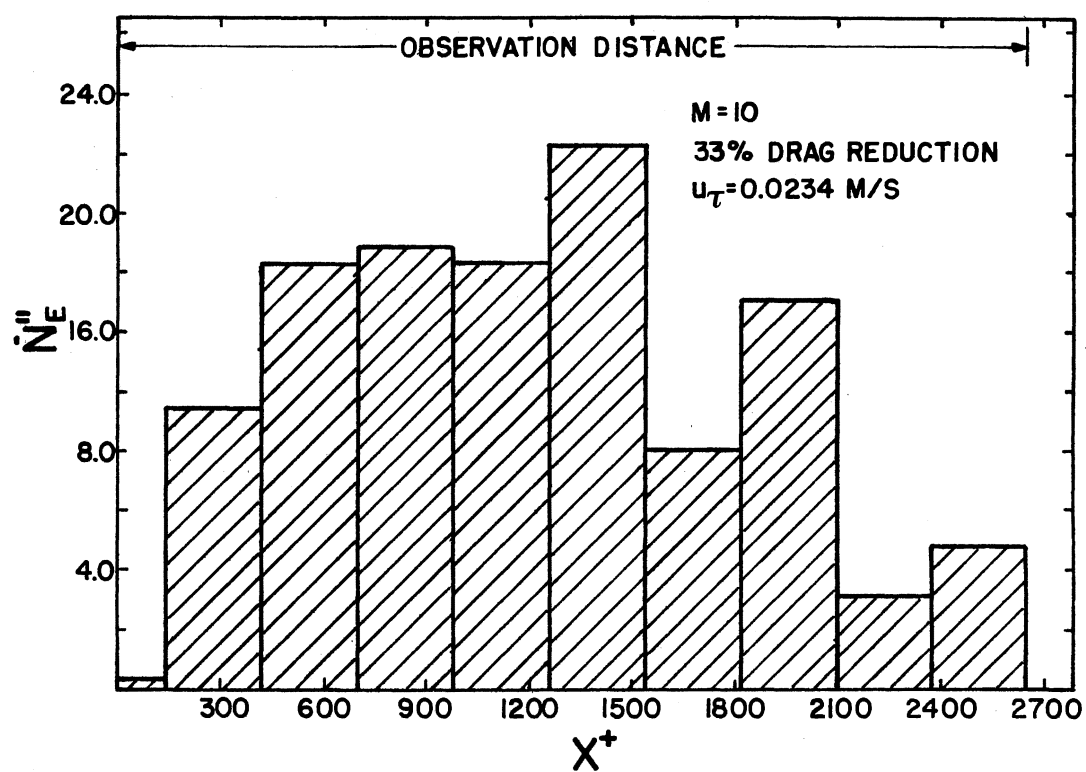


Figure 2. Histogram of Ejection Rate/Unit Area as a Function of Downstream Distance for Drag Reducing Flow, 33% D.R., $M = 10$

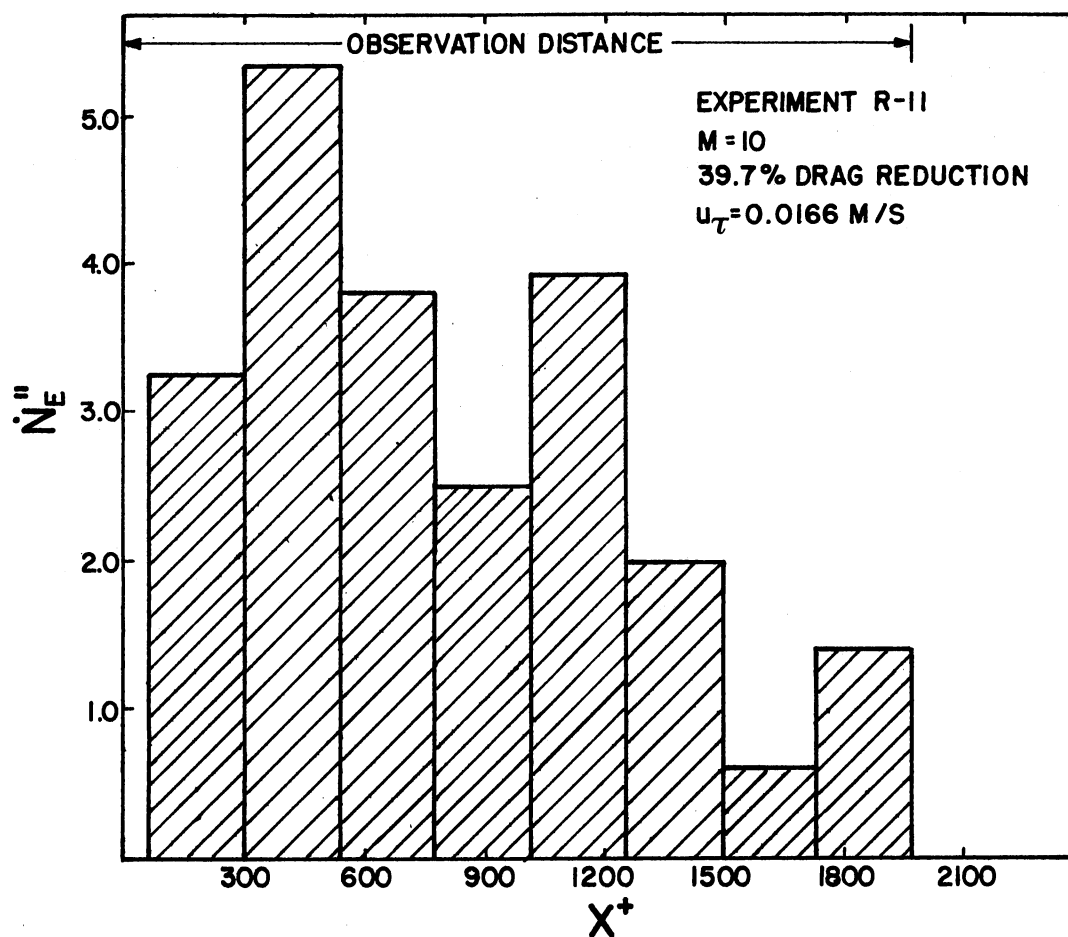


Figure 3. Histogram of Ejection Rate/Unit Area as a Function of Downstream Distance for Drag Reducing Flow, 39.7% D.R., M = 10

APPENDIX B

UNCERTAINTY ESTIMATES

The experimental uncertainty estimates used in this study were made using the method developed by Kline and McClintock (12). The major sources of uncertainty in this study are in the measurement of:

1. Mass averaged channel velocity.
2. Average channel wall shear velocity.
3. Momentum and displacement thicknesses.
4. Viscosity measurements.
5. Bursting measurement periods.

Mass Averaged Channel Velocity

The mass averaged flow rate, \dot{Q} , equals a collected volume, V , divided by the collection time, T .

$$\frac{\Delta \dot{Q}}{\dot{Q}} = \left[\left(\frac{\Delta V}{V} \right)^2 + \left(\frac{\Delta T}{T} \right)^2 \right]^{1/2}.$$

The calculated uncertainties range from $\pm 1\%$ to $\pm 1.8\%$.

Average Channel Wall Shear Velocity

From a force balance on a bounded volume of fluid:

$$u_{\tau}^2 = - \frac{D}{4\rho} \frac{dp}{dz}$$

$$\frac{\Delta u_{\tau}}{u_{\tau}} = \left[\left(\frac{1}{2} \frac{\Delta P}{P} \right)^2 + \left(\frac{1}{2} \frac{\Delta z}{z} \right)^2 + \left(\frac{1}{2} \frac{\Delta \rho}{\rho} \right)^2 + \left(\frac{1}{2} \frac{\Delta D}{D} \right)^2 \right]^{\frac{1}{2}}.$$

The computed wall shear velocity uncertainties ranged from 0.6% to 1.2%.

Momentum and Displacement Thicknesses

U and U_{ζ} were estimated using a computer velocity profile program successfully developed by Reischman (23). His estimates in the uncertainty of U and U_{ζ} are approximately 5.5% in flows of similar Reynolds number and composition. This would result in

$$\frac{\Delta \theta}{\theta} = \pm 17.4\%; \quad \frac{\Delta \delta^*}{\delta^*} = \pm 7.8\%.$$

Viscosity Measurements

The smallest reading on the Brookfield Viscometer scale was 0.1. Using this number as a reference to calculate uncertainty:

$$\frac{\Delta v}{v} = \pm 0.5\%.$$

Bursting Measurement Periods

The uncertainty calculated in the method II bursting period measurements resulted from using a 95% confidence interval of a test statistic from either a student t distribution or a normal distribution. The distribution choice was based on the number of burst periods sampled and the sample mean and variance.

APPENDIX C

TABLES

This appendix contains the tables referred to in the text of this thesis.

TABLE I
PREVIOUS INVESTIGATIONS RELATED TO THE BURSTING PROCESS

Ejection Periods ($T_e = d_s / N_e \lambda$)	Bursting Periods ($T_b = d_s / N_b \lambda$)	Ejection Periods (Visual)	Bursting Periods (Visual)	Conditional Sampling Hot-Wire Periods
Achia (1)	Present Measurements	Kim et al. (11)	Offen and Kline (19)	Kim et al. (11)
Donohue et al. (5)				Lu and Willmarth (16)
Kline et al. (13)				Meek (17)
				Rao et al. (22)
				Wallace et al. (27)
				Present Measure- ments

TABLE II
POLYMER VISCOSITY RATIOS

Experiment Set	Solution	Ratio	Shear Rate
R-6	50 wppm AP 273	1.30	73 sec ⁻¹
R-9	100 wppm TR0 323	1.54	73 sec ⁻¹
R-11	50 wppm AP 273	1.40	73 sec ⁻¹

TABLE III
FLOW CONDITIONS UNCERTAINTIES: 19:1 ODDS

Film Set	Wall Shear Velocity (m/s)	Mass Averaged Velocity (m/s)	Kinematic Viscosity (m^2/s) $\times 10^{-6}$	Momentum Thickness (cm)	Displacement Thickness (cm)
R-8	0.0173 ± 0.0017	0.3139 ± 0.0024	1.310 ± 0.01	0.2173 ± 0.0169	0.335 ± 0.058
R-12	0.01725 ± 0.0017	0.3079 ± 0.00244	1.352 ± 0.01	0.219 ± 0.017	0.344 ± 0.060
R-12	0.02048 ± 0.0015	0.3493 ± 0.0052	1.352 ± 0.01	0.222 ± 0.017	0.335 ± 0.059
R-12	0.02078 ± 0.0016	0.3627 ± 0.0052	1.352 ± 0.01	0.219 ± 0.017	0.322 ± 0.058
R-6	0.01581 ± 0.0019	0.2887 ± 0.0035	1.799 ± 0.01	--	--
R-9	0.0234 ± 0.0014	0.4075 ± 0.0091	2.127 ± 0.01	0.212 ± 0.017	0.369 ± 0.064
R-9	0.02078 ± 0.0015	0.4075 ± 0.0064	2.127 ± 0.01	0.222 ± 0.017	0.379 ± 0.066
R-11	0.01683 ± 0.0019	0.3780 ± 0.0055	1.778 ± 0.01	0.225 ± 0.018	0.402 ± 0.070
R-11	0.01661 ± 0.0018	0.3688 ± 0.0055	1.778 ± 0.01	0.226 ± 0.018	0.403 ± 0.070

TABLE IV
FLOW CONDITIONS UNCERTAINTIES: 19:1 ODDS

Film Set	Wall Shear Velocity (m/s)	Center Line Velocity (m/s)	Temperature °C	Percent Drag Reduction	Solution
R-8	0.0173 ±.0017	0.3627 ±.0046	10.0 ±.3	0	Water
R-12	0.01725 ±.00017	0.3563 ±.0046	8.9 ±.3	0	Water
R-12	0.02048 ±.00015	0.4030 ±.0073	8.9 ±.3	0	Water
R-12	0.02078 ±.00016	0.4179 ±.0073	8.9 ±.3	0	Water
R-6	0.01581 ±.00019	--	8.9 ±.3	17.25	50 wppm AP 273
R-9	0.0234 ±.00014	0.6032 ±.0122	8.3 ±.3	33.00	100 wppm TR0 323
R-9	0.02078 ±.00015	0.4795 ±.0088	8.3 ±.3	16.60	100 wppm TR0 323
R-11	0.01683 ±.00019	0.4500 ±.0076	9.4 ±.3	40.90	50 wppm AP 273
R-11	0.01661 ±.00018	0.4389 ±.0079	9.4 ±.3	39.70	50 wppm AP 273

TABLE V
FLOW DATA USED IN EVALUATING BURSTING MEASUREMENTS BY ACHIA

Run No.	Drag Reduction	Wall Shear Velocity (m/s)	Centerline Velocity (m/s)	Displacement Thickness (cm)	Momentum Thickness (cm)
W1	0%	.0152	.326	.196	.120
W2	0%	.0239	.524	.175	.116
W3	0%	.0325	.689	.171	.118
S1	20%	.0218	.533	.198	.117
S2	32%	.0256	.695	.189	.112
S3	44%	.0343	1.020	.169	.150

TABLE VI
FLOW DATA USED IN EVALUATING DONOHUE ET AL. BURSTING MEASUREMENTS

Drag Reduction	Wall Shear Velocity (m/s)	Centerline Velocity (m/s)	Displacement Thickness (cm)	Momentum Thickness (cm)
0%	.0073	.168	.402	.231
0%	.0011	.243	.343	.216
0%	.0011	.241	.358	.221
16%	.0067	.169	.528	.262
28%	.0095	.256	.454	.241
33%	.0092	.259	.509	.256

TABLE VII
BURSTING MEASUREMENT METHOD I

Film Set	Wall Shear Velocity (m/s)	Percent Drag Reduction	Dye Slot Width (cm)	Observation Time (sec)	Total Bursts Counted	Downstream Observation Distance (cm)	$T_b = d_s / \dot{N} \lambda$ (sec)
R-8	0.01730	0	0.889 1.2λ	16.8	76	17.80	0.2600
R-12	0.01725	0	0.076 $\lambda/10$	129.3	370	15.25	0.0340
R-12	0.02079	0	0.660 0.98λ	64.7	350	15.25	0.1870
R-12	0.02048	0	0.076 $\lambda/8.7$	64.6	240	15.25	0.0311
R-9	0.02340	33.0	1.651 0.96λ	30.7	154	38.10	0.2240
R-11	0.01660	39.7	2.235 1.19λ	38.5	86	53.30	0.5260
R-11	0.01680	40.9	0.254 $\lambda/9$	45.5	75	12.7 to 40.6	0.1290

TABLE VIII
BURSTING MEASUREMENT METHOD II

Film Set	Wall Shear Velocity (m/s)	Percent Drag Reduction	Dye Slot Width	Real Time (sec)	Total Bursts Counted	Downstream Observation Point (cm)	T _b (sec)	T _d (sec)
R-8	0.01730	0	1.2 λ	34.6	32	4.45	1.010 \pm .250	0.930 \pm .32
R-12	0.01725	0	$\lambda/10$	129	135	3.81	1.030 \pm .180	0.410 \pm .074
R-12	0.02048	0	$\lambda/8.7$	64.5	92	3.81	0.694 \pm .075	0.350 \pm .066
R-12	0.02078	0	0.98 λ	64.4	101	3.81	0.638 \pm .101	0.397 \pm .109
R-9	0.02340	33.0	0.96 λ	32.2	24	13.97	1.310 \pm .331	1.140 \pm .483
R-9	0.02078	16.6	$\lambda/6.3$	47.4	47	13.97	0.973 \pm .153	0.530 \pm .160
R-11	0.01660	39.7	0.98 λ	36.9	27	13.97	1.320 \pm .310	0.780 \pm .310
R-11	0.01680	40.9	$\lambda/9$	69.6	55	13.97	1.260 \pm .140	0.930 \pm .220
All Uncertainties at 19:1 Odds								

TABLE IX
DOWNSTREAM VIEWING LENGTHS USED IN DYE VISUALIZATION EXPERIMENTS

Maximum Field of View (X^+)	Type of Flow	Investigator
1945 to 2343	Water	Present Measurements
972 to 2569	Water	Donohue et al. (5)
1064 to 2275	Water	Achia (1)
4191 (33% D.R.) to 5045 (39.7% D.R.)	Polymer	Present Measurements
1086 (16% D.R.) to 1298 (33% D.R.)	Polymer	Donohue et al. (5)
1090 (20% D.R.) to 1725 (44% D.R.)	Polymer	Achia (1)

APPENDIX D

FIGURES AND ILLUSTRATIONS

This appendix contains the figures and illustrations referred to in the text of this thesis.

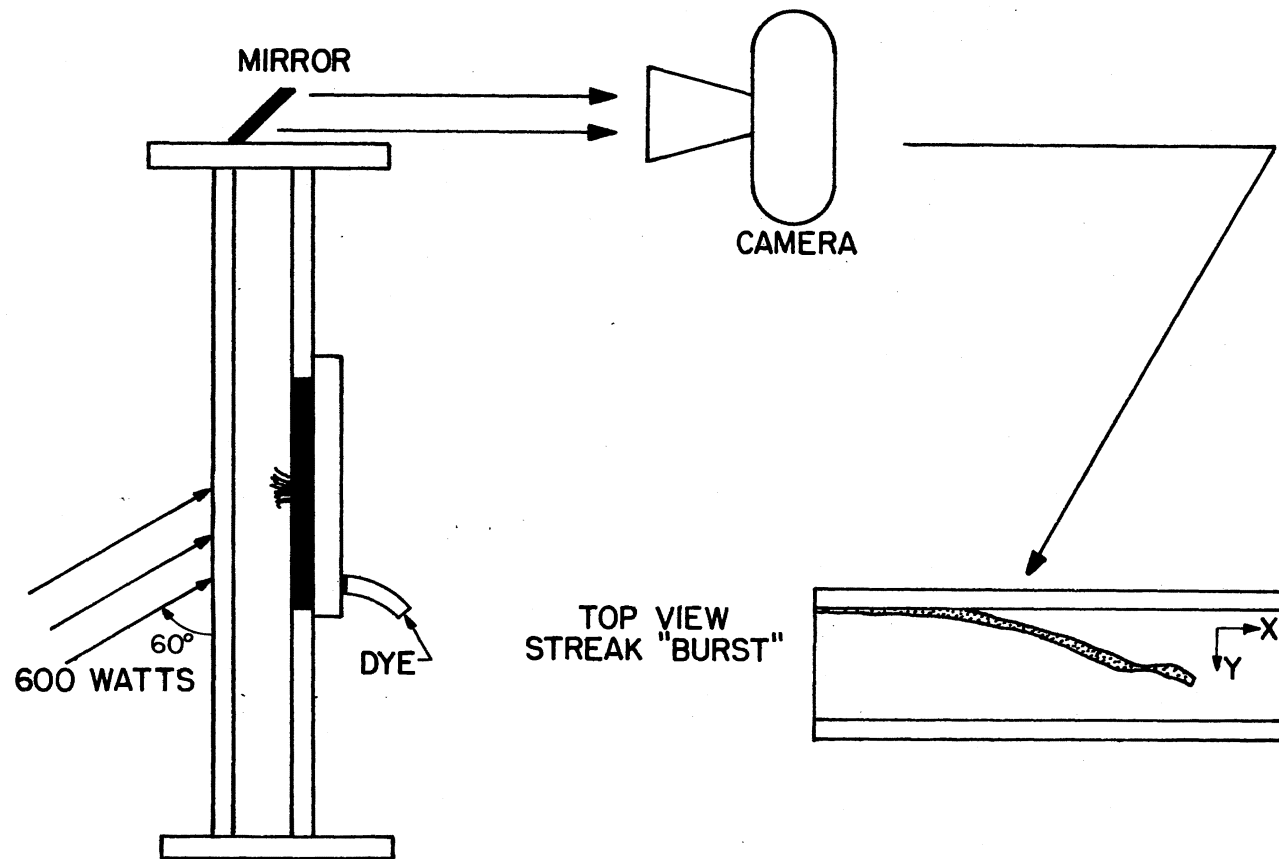


Figure 5. End View of Flow Channel Illustrating Mirror and Light-
ing Arrangement Used in Experiments

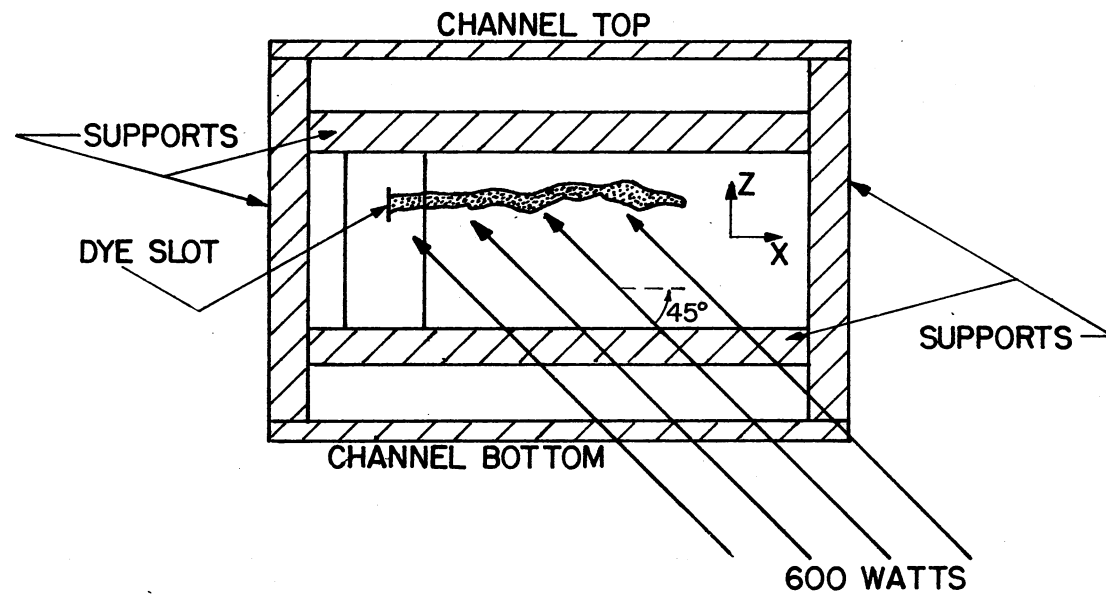


Figure 6. Side View of Flow Channel Illustrating Maximum Lighting Angle With Channel Wall to Achieve Minimum Glare in Picture

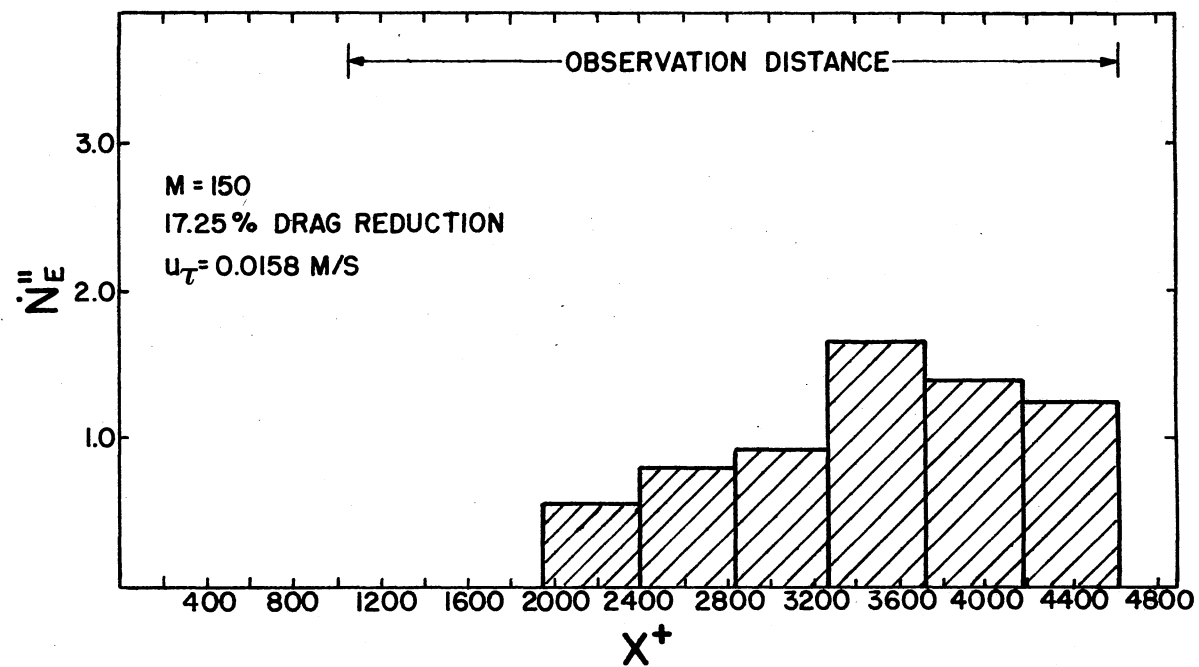


Figure 7. Histogram of Ejection Rate/Unit Area as a Function of Distance Downstream of Dye Slot for Drag Reducing Flow at $M = 150$

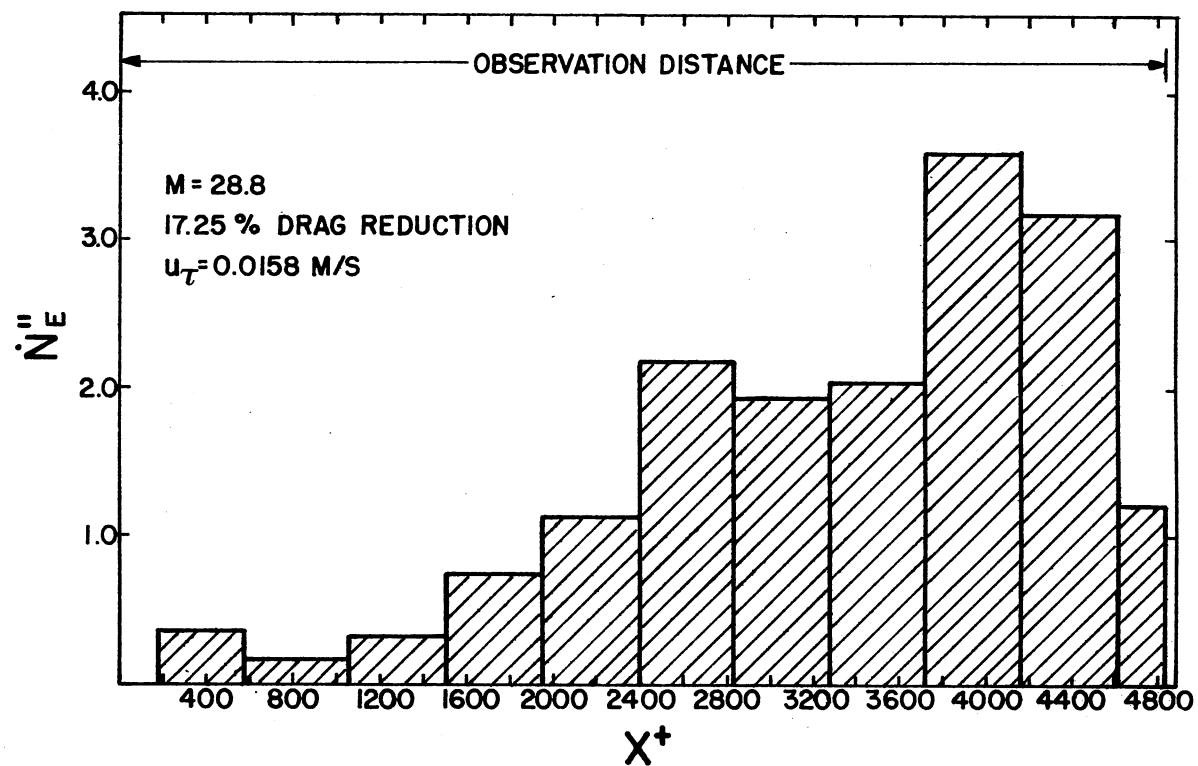


Figure 8. Histogram of Ejection Rate/Unit Area as a Function of Distance Downstream of Dye Slot for Drag Reducing Flow at $M = 28.8$

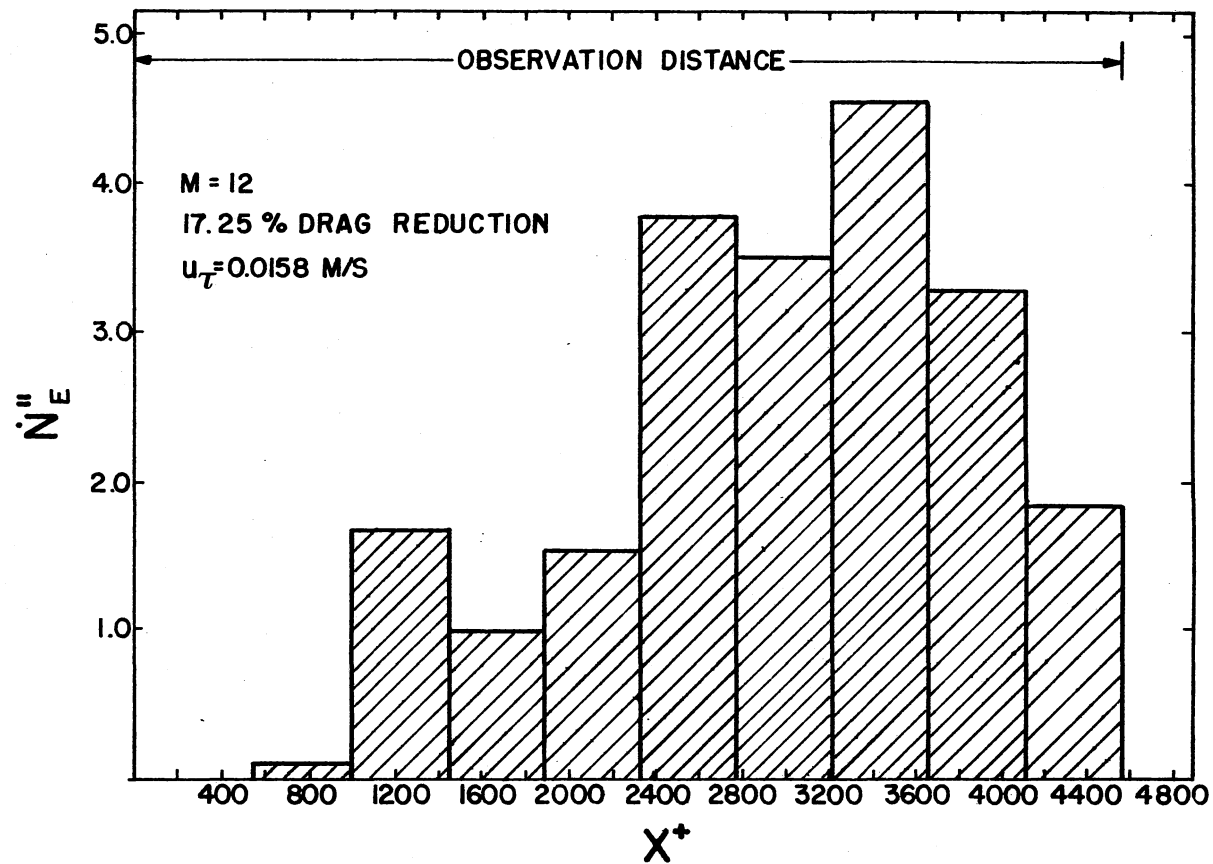


Figure 9. Histogram of Ejection Rate/Unit Area as a Function of Distance Downstream of Dye Slot for Drag Reducing Flow at $M = 12$

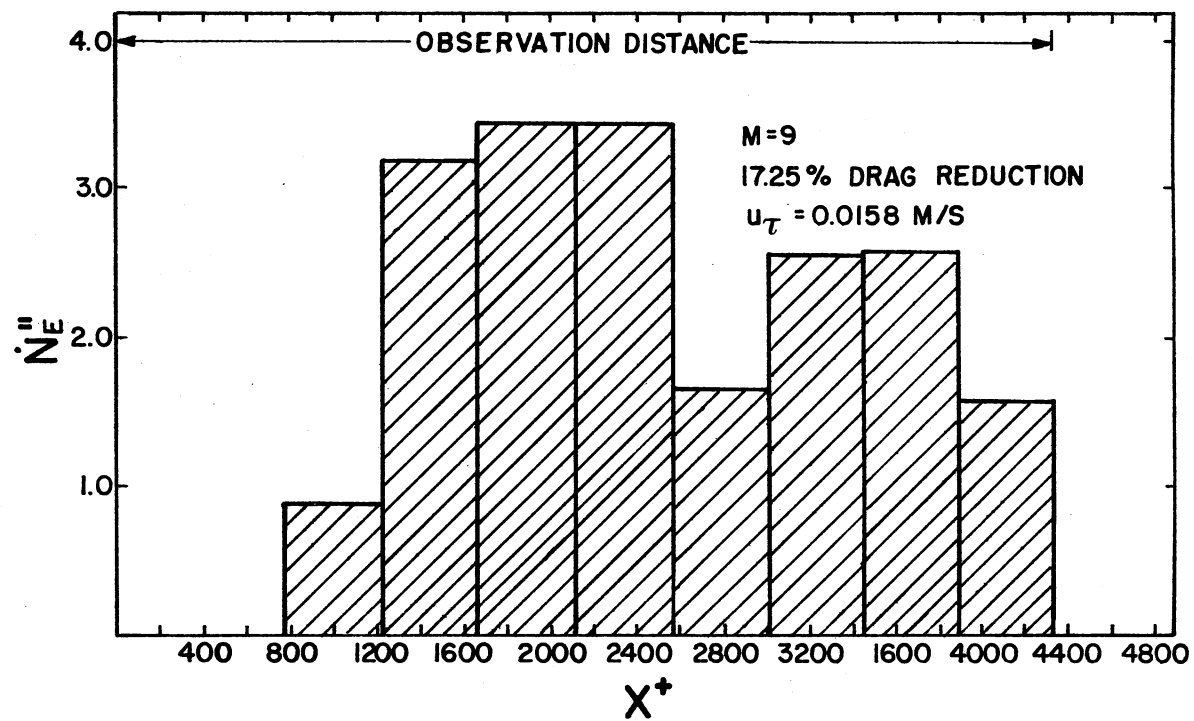


Figure 10. Histogram of Ejection Rate/Unit Area as a Function of Distance Downstream of Dye Slot for Drag Reducing Flow at $M = 9$

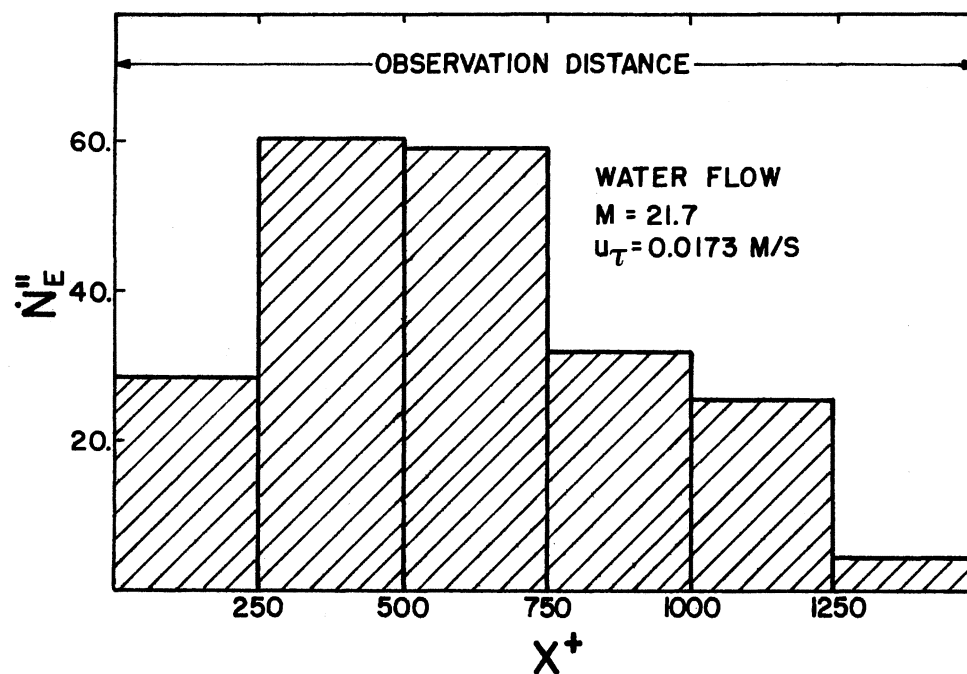


Figure 11. Histogram of Ejection Rate/Unit Area as a Function of Distance Downstream of Dye Slot for Water Flow at $M = 21.7$

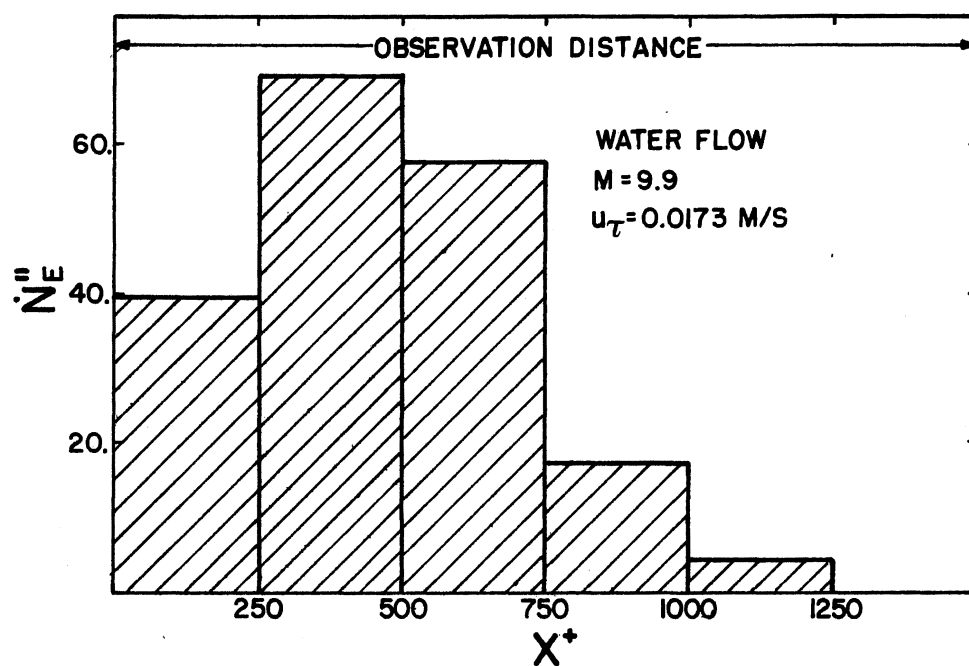


Figure 12. Histogram of Ejection Rate/Unit Area as a Function of Distance Downstream of Dye Slot for Water Flow at $M = 9.9$

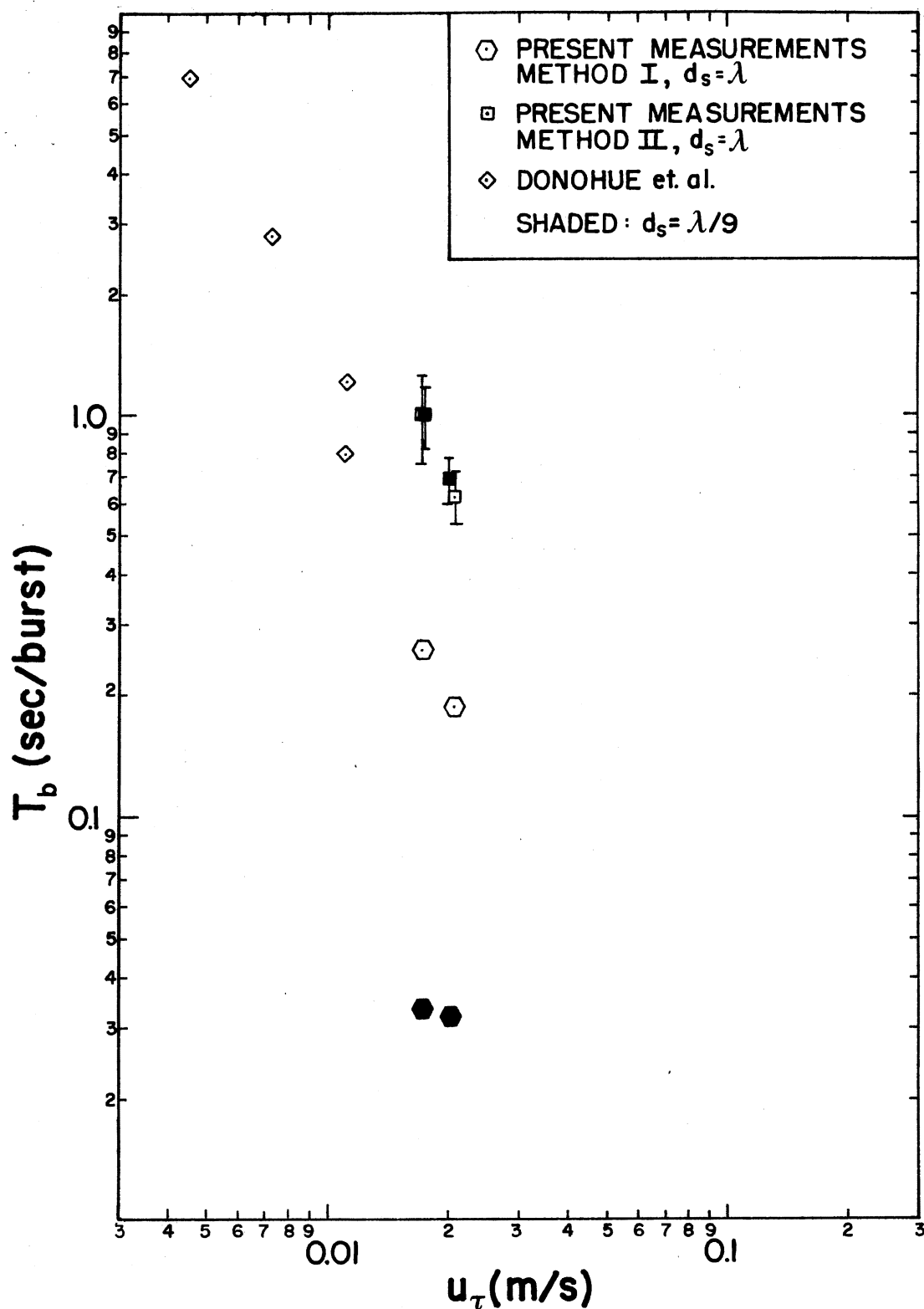


Figure 13. Bursting Period Measurements Made in Water at the Oklahoma State University Experimental Facility

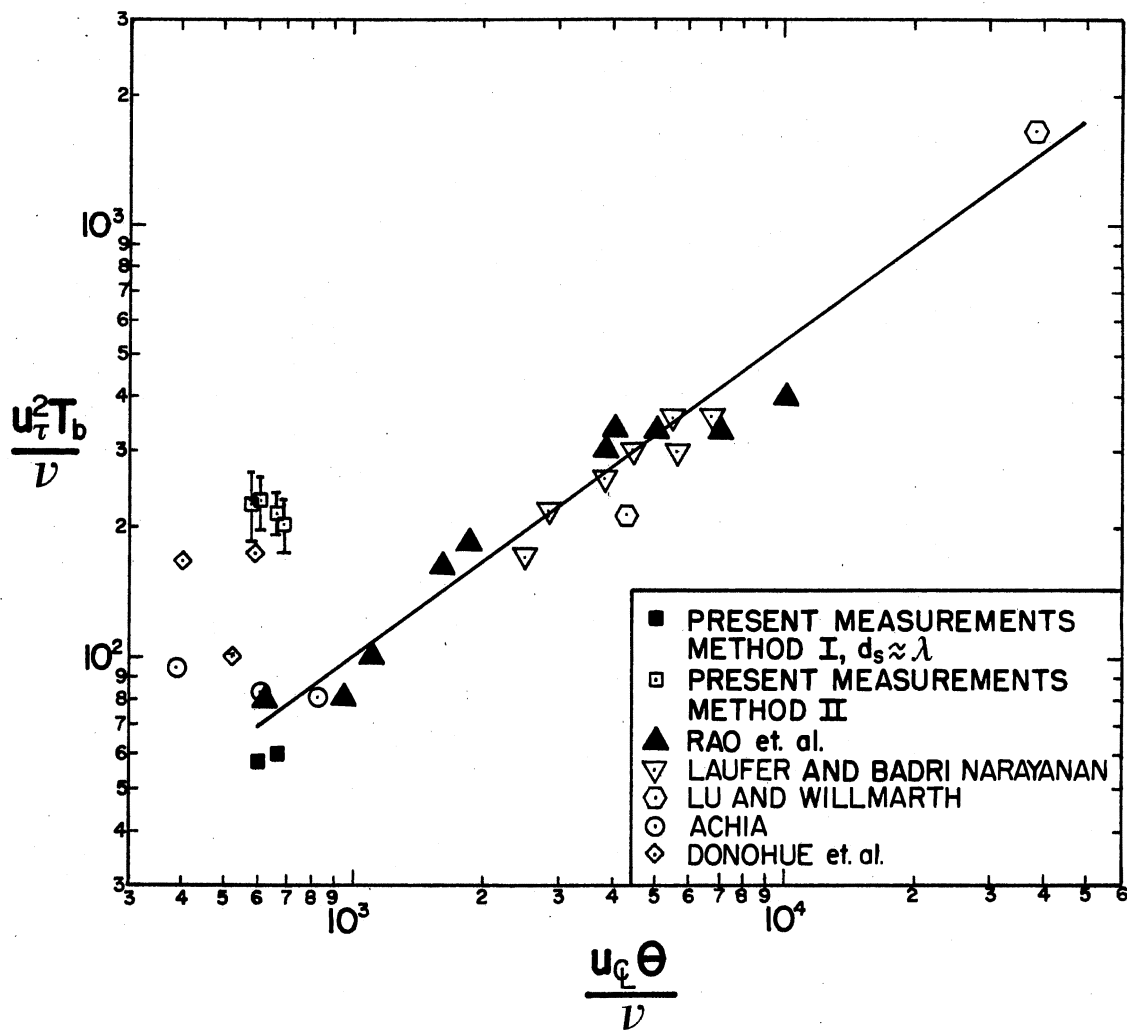


Figure 14. Bursting Periods in Newtonian Flows Normalized With Inner Flow Variables, u_τ and ν

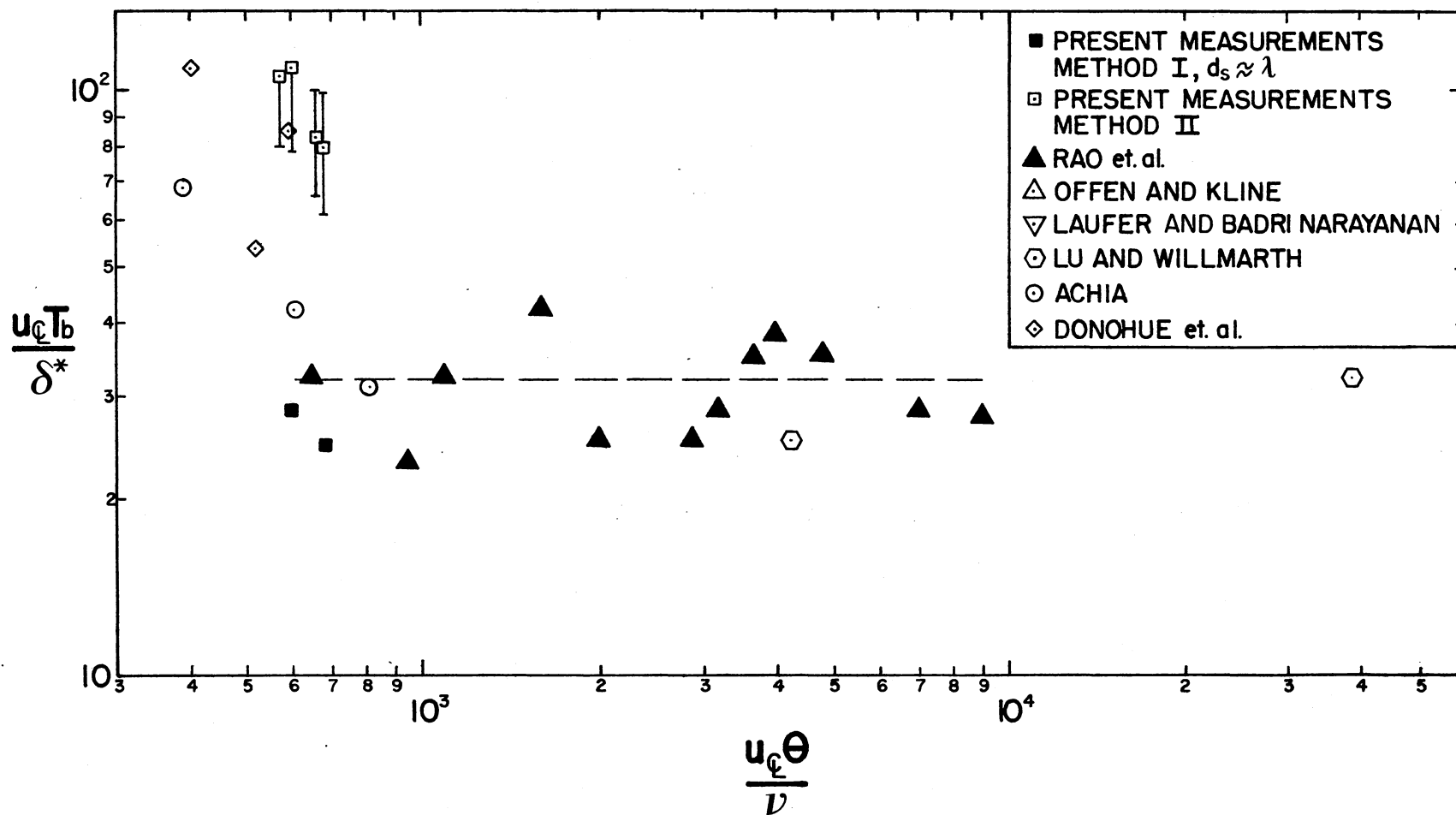


Figure 15. Bursting Periods in Newtonian Flows Normalized With Outer Flow Variables, u_{ℓ} and δ^*

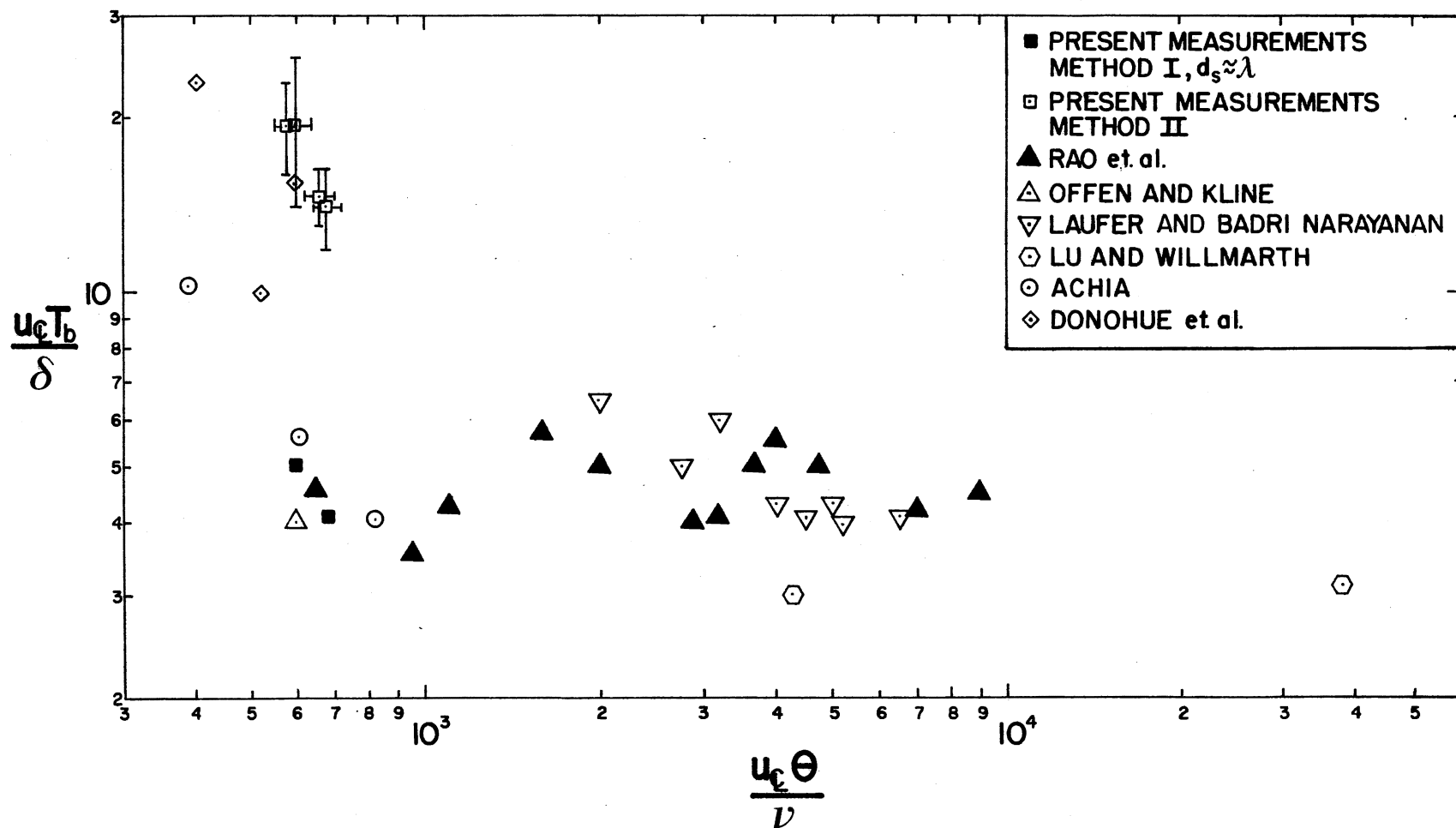


Figure 16. Bursting Periods in Newtonian Flows Normalized With Outer Flow Variables, u_{ℓ} and δ

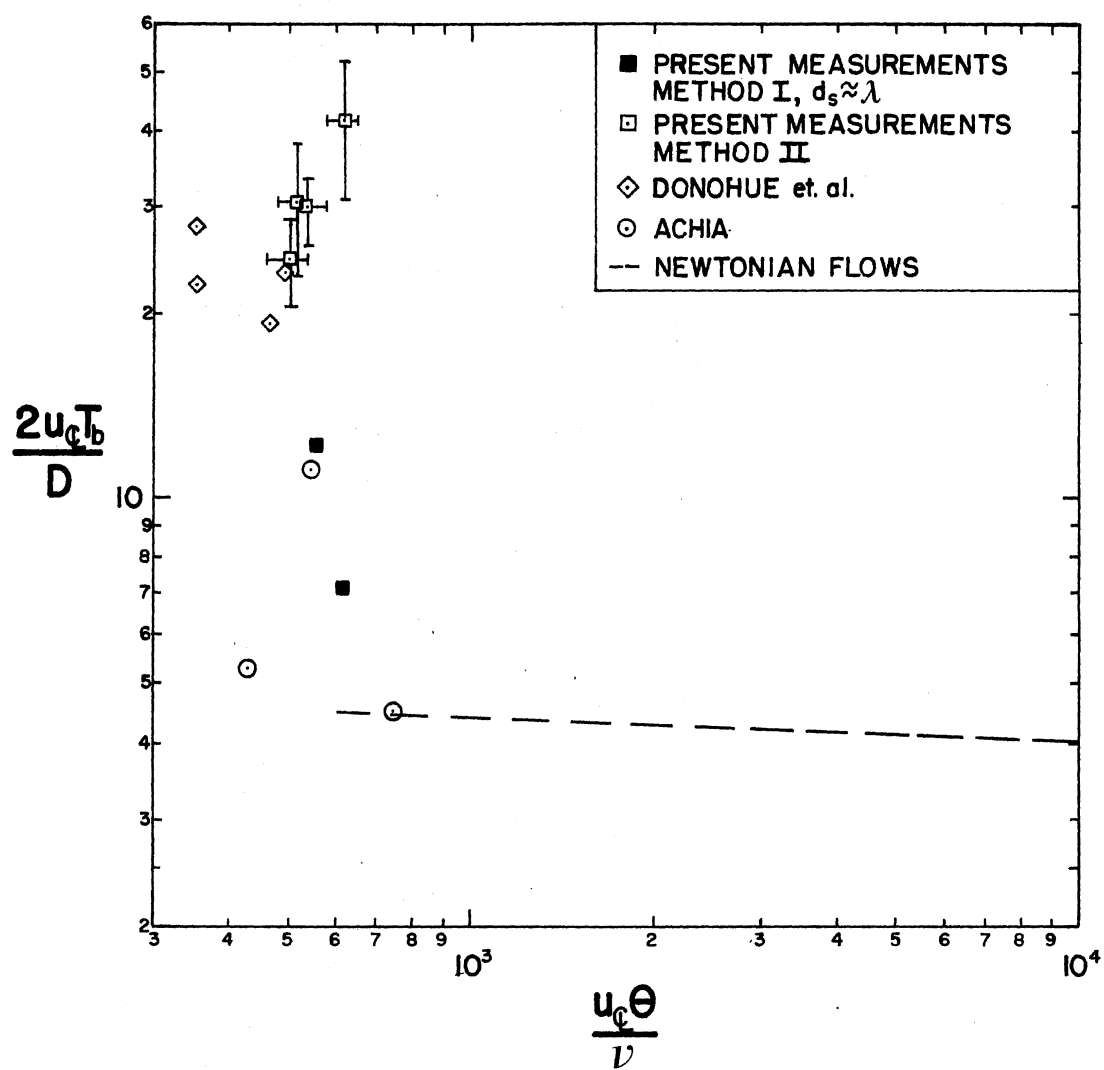


Figure 17. Bursting Periods in Drag Reducing Flows Normalized With Outer Flow Variables, $u_{c,\theta}$ and $D/2$

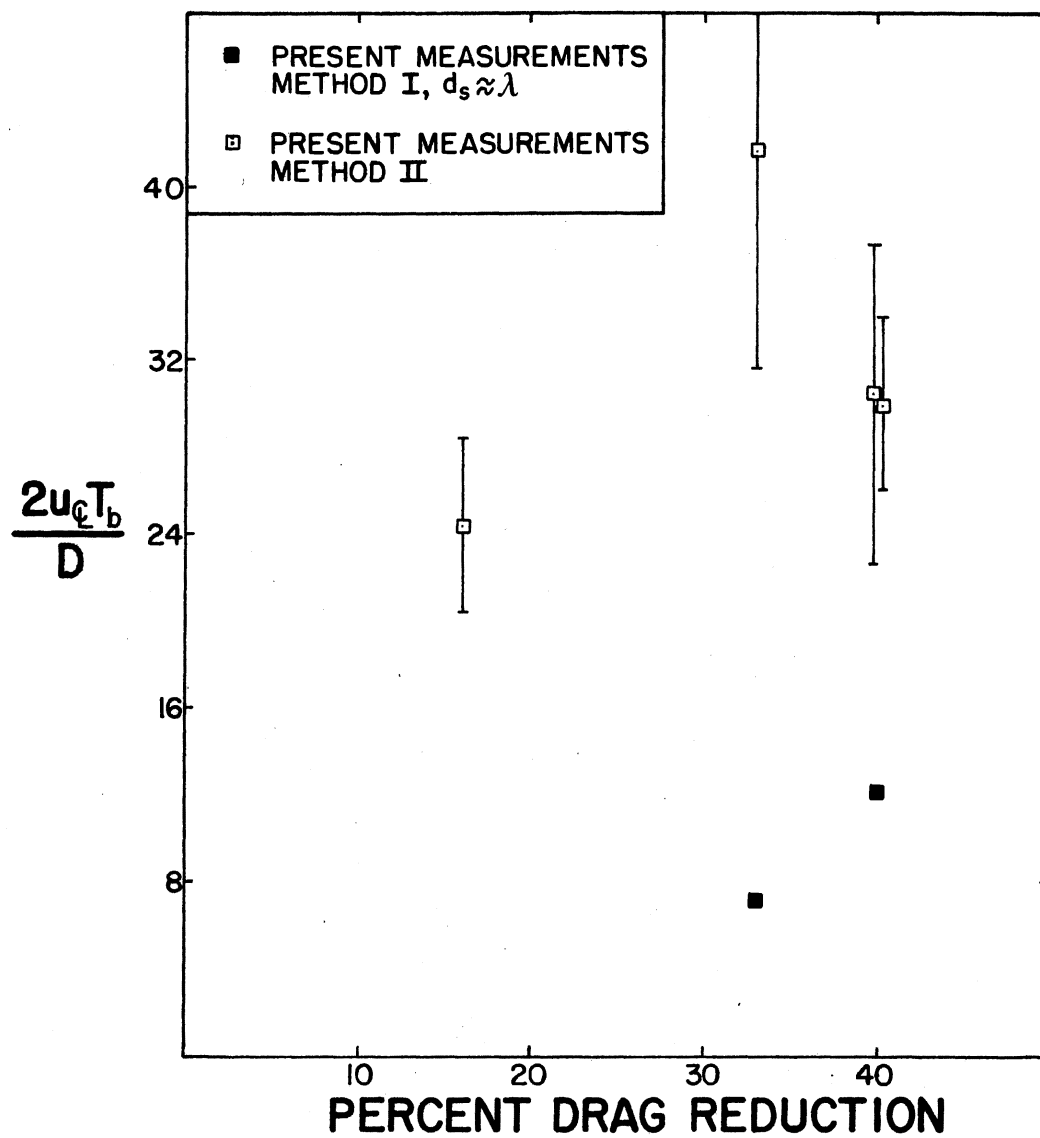


Figure 18. Present Bursting Period Measurements as a Function of the Amount of Drag Reduction Occurring in the Flow

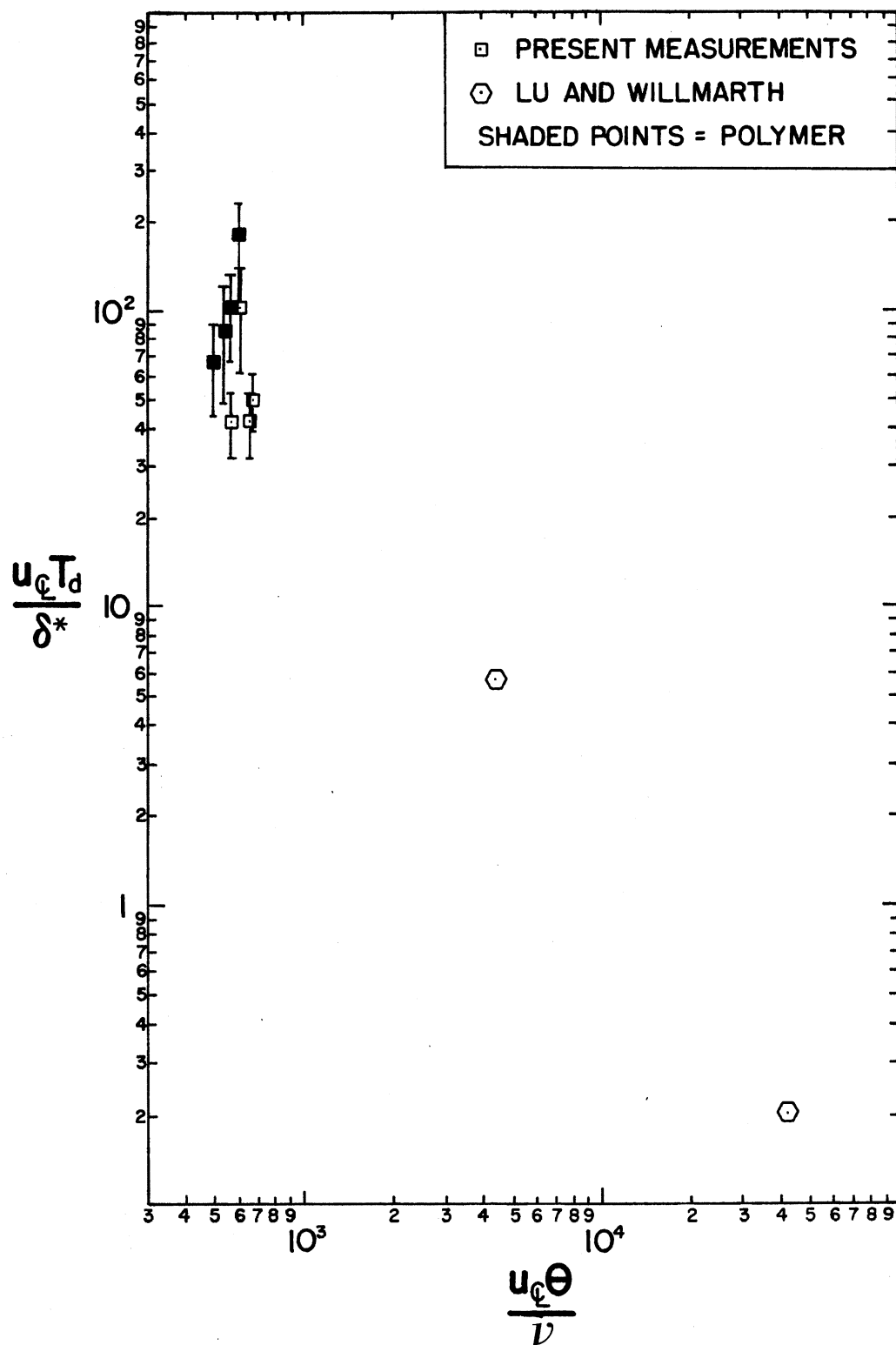


Figure 19. Bursting Duration Normalized With Outer Flow Variables, u_L and δ^*

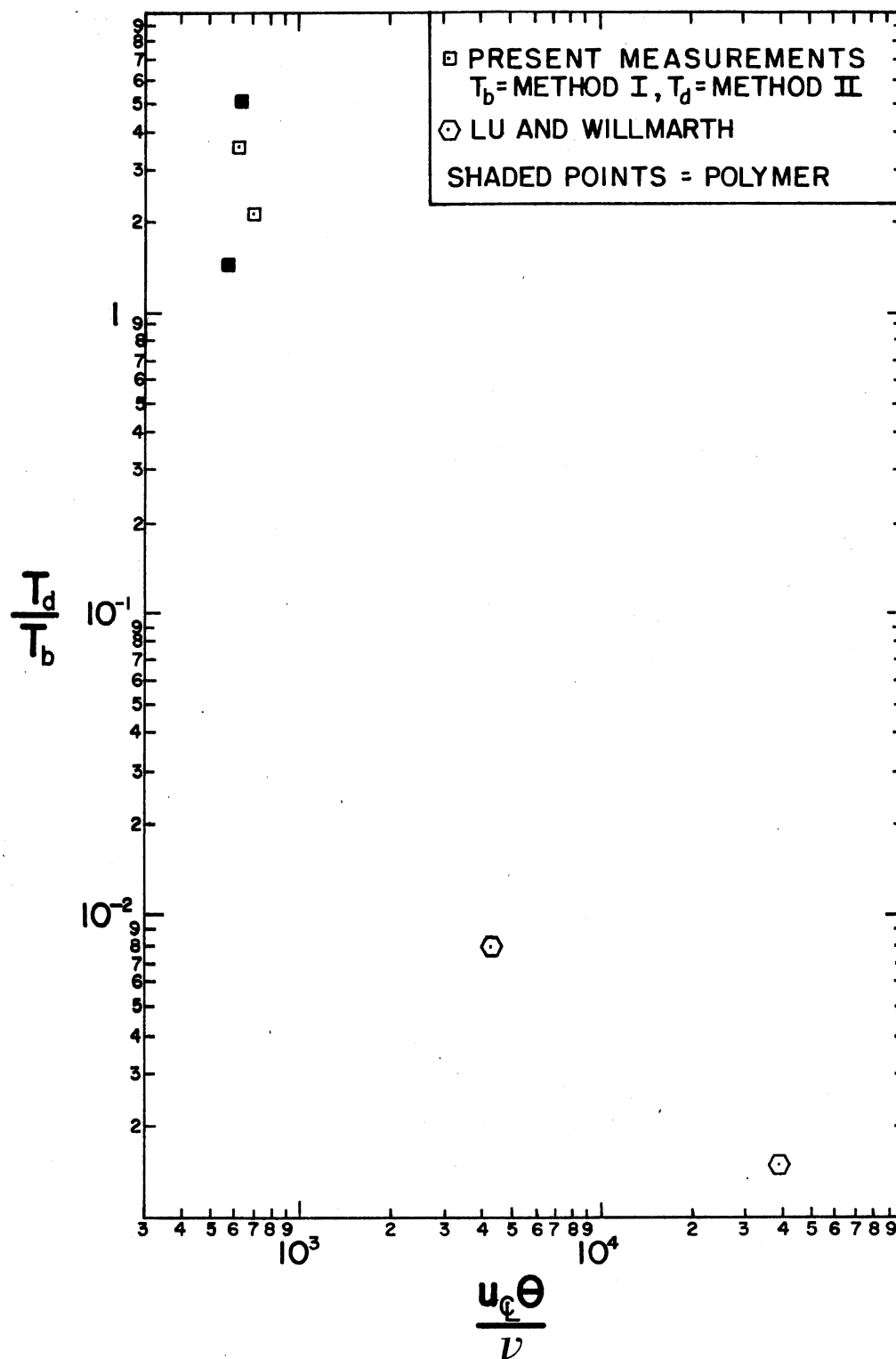


Figure 20. Ratio of Bursting Duration to Bursting Period

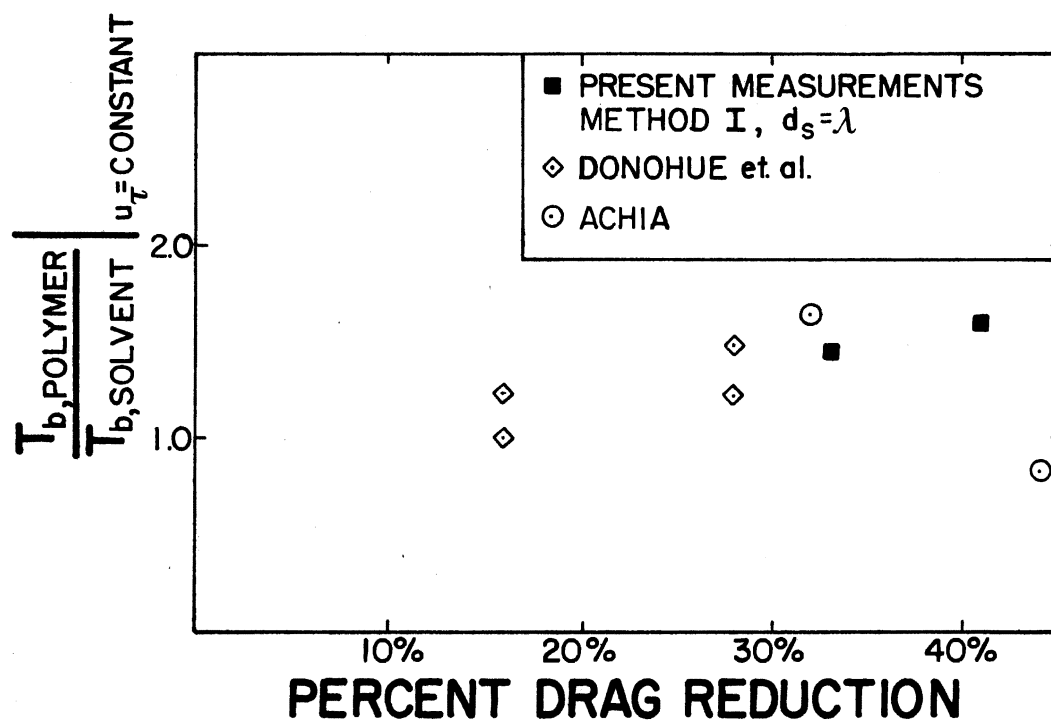


Figure 21. Ratio of Polymer and Solvent Bursting Periods for Measurement Method I as a Function of Drag Reduction

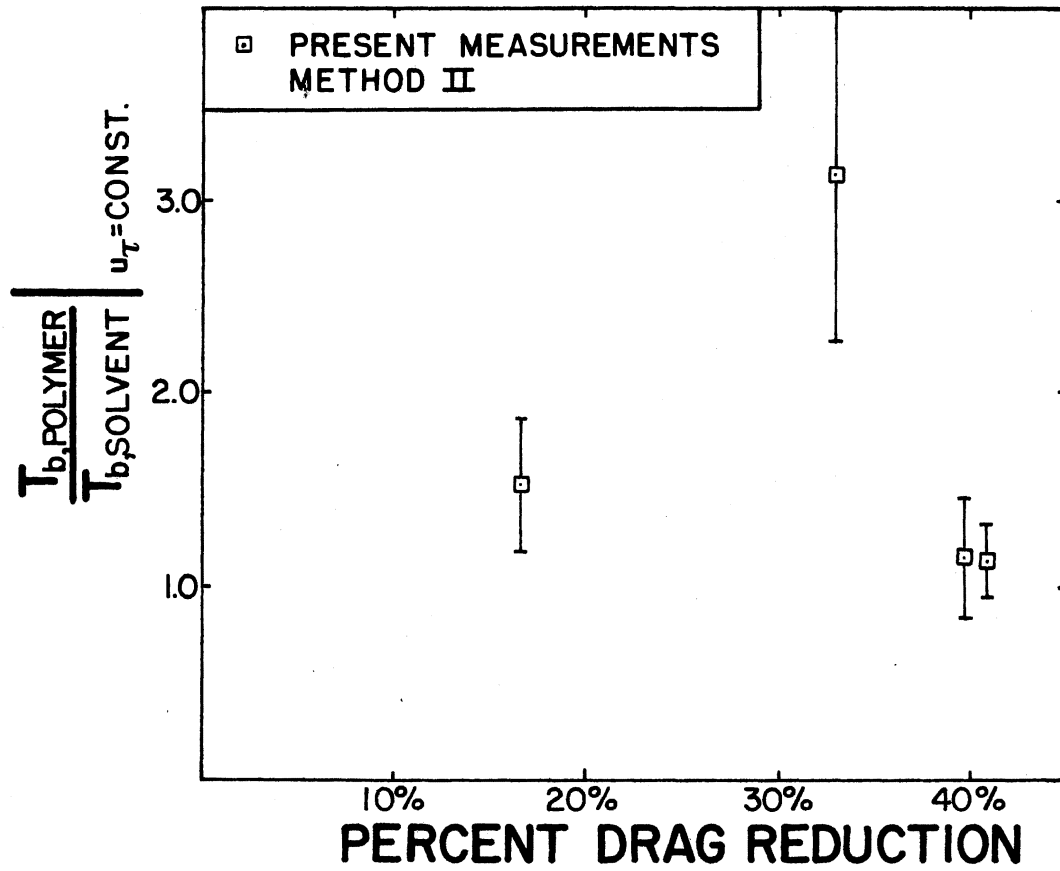


Figure 22. Ratio of Polymer and Solvent Bursting Periods for Measurement Method II as a Function of Drag Reduction

VITA^α

Alan Jackson Smith

Candidate for the Degree of

Master of Science

Thesis: AN INVESTIGATION OF THE BURSTING EVENTS IN DRAG REDUCING
TURBULENT CHANNEL FLOWS

Major Field: Mechanical Engineering

Biographical:

Personal Data: Born in Huron, South Dakota, July 19, 1951, the son
of Mr. and Mrs. Earl B. Smith.

Education: Graduated from Midwest City High School, Midwest City,
Oklahoma, May, 1969; received the Bachelor of Science degree
in Mechanical Engineering, Oklahoma State University, 1973;
completed the requirements for the Master of Science degree
at Oklahoma State University, December, 1975.

Professional Experience: Engineering Aid, Lawrence Livermore Labora-
tories, Summer, 1972; Engineering Aid, Collins Engineering
Associates, Summer, 1973; Engineer, Halliburton Services,
Summer, 1974; Graduate Research and Teaching Assistant,
Oklahoma State University, 1974-75; Mechanical Engineer,
Brown and Root, Inc., 1975.